Mestrado Integrado em Engenharia Química

Influence of cross linking degree of a PDMS network in the size of the pores of a selectively etched PDMS-PMMA Interpenetration Networks

Master thesis

Desenvolvido no âmbito da disciplina de

Projecto de Desenvolvimento em Instituição Estrangeira

Ana Maria Curado Mateus Correia

Departamento de Engenharia Química

Arguente na FEUP: **Prof. PhD.Fernão Magalhães**
Orientador na Instituição Estrangeira: **Prof. PhD Martin Vigild**
PhD Sokol Ndoni

Março de 2009

Acknowledgments

Firstly I would like to thank all the Nanoporous Group, Martin Vigild, Sokol Ndoni, Lars Schulte, Fengxiau Guo, Li Li, Kaushal Sagar, Piotr Szewczkowski for welcoming me and making me feel so comfortable. Especially I would like to thank to Martin and Sokol, for all their comments and support, to Fengxiao, for helping me with the SAXS experiments and for being always available to discuss my doubts and to Lars for helping me with the preparation of the samples for the microscopy.

I also want to thank to my family and friends in Portugal that, in spite the distance always remained very close.

And finally, I would like to thank to my "Danish family", Audrey, Caroline, Daniela, David, Samuel and Sara for making my staying in Denmark an incredible adventure.

Resumo

Os materiais nanoporosos podem ser produzidos através da remoção selectiva de um bloco, num dibloco copolimero. Esta técnica acarreta algumas desvantagens, ou inconvenientes, devido ao tempo excessivo necessário à criação de copolimers, tornando-se, desta forma, um processo demasiado caro e lento para ser aplicado industrialmente. De forma a responder aos requisitos necessários de aplicabilidade industrial foi desenvolvido um novo método para a criação de materiais polimericos nanoporosos, a partir de "*interpenetration networks"* (IPN). Esta técnica pode ser dividida em três partes começando pela criação de uma *matriz hospedeira,* seguindo-se a formação de uma IPN através da polimerização de uma *matriz hóspede* dentro da *matriz hospedeira.* Finalmente, a criação de materiais nanoporosos é feita a partir da remoção selectiva da *matriz hospedeira*.

Neste trabalho, a criação de um material nanoporoso foi realizada com o método IPN e a influência do grau de *cross-link* de uma matriz the poli-dimetil-siloxane (PDMS), "*matriz hospedeira*", no tamanho dos nanoporos foi estudada.

De forma a estudar o efeito da percentagem de "*cross-linker"* no polímero a ser removido, no tamanho dos poros, várias experiencias foram realizadas a três amostras com diferentes graus de *"cross-link"* (40 mol%, 60 mol% and 75 mol%). Entre as técnicas usadas para comparar o tamanho dos poros foram realizadas medições gravimétricas, FTIR, SAXS e microscopia, como TEM e SEM.

Contrariamente ao que se esperava inicialmente, o grau de ligações da *"matriz hospedeira"* parece não influenciar o tamanho dos poros do material poroso obtido.

Abstract

Nanoporous materials can be produced by selectively removing one polymer block from a di-block copolymer. This technique has some disadvantages due to the time consuming method used to produce the copolymers, becoming, therefore, a very expensive process to be applied industrially. In order to meet the requirements for an industrial application, a interpenetration networks (IPN) method, instead of di-block copolymers, was used. This technique can be divided in 3 main stages beginning with the creation of host network, followed by creation of IPN by polymerizing the guest network within the host matrix, and finally the creation of the nanoporous material by etching the host polymer network.

In this work the IPN method was used and the influence of the cross-linking degree of Polydimethylsiloxane network (PDMS), the host network, on the size of the nanopores was studied.

In order to study the effect of the cross-linker of the etchable network (PDMS) in the size of the pores, several experiments, such as Gravimetric measurements, swelling measurements, FT-IR, SAXS and microscopy, like TEM and SEM were done to three samples with different amounts of cross-linker (40 mol%, 60 mol% and 75 mol%).

Unlike what was expected initially, the cross-linking degree seems to not affect the size of the pores of the obtained porous material.

This research took place in the Danish Polymer Center (Technical University of Denmark).

Table of Contents

List of Figures

List of Tables

Abbreviations

D	Diameter of the Petri dish	m
T	Thickness	m
M_n	Number Average Molecular Weight	
M_w	Weight Average Molecular Weight	
PDI	Poly Dispersion Index ($PDI=M_w/M_n$)	
w	Weight	g
FT-IR	Fourier Transformation Infrared	
SAXS	Small Angle X-ray Scattering	
(SDAs)	Structure directing agents	

Greek Letters

P	Volumetric Mass	g/dm^3

List of reactants

A	AIBN	Azobisisobutyronitrile
D	DCP	Dicumyl Peroxide
	DEGMA	Diethyleneglycoldimethacrylate
H	HF	Hidrogenfluoride
I	IPN	Interpenetrating Network
M	MMA	Methylmethacrylate
N	NPM	Nanoporous Material
P	PDMS	Polydimethylsiloxane
	PMMA	Polymethylmethacrylate
T	TBAF	Tetrabutylammonium fluoride
	TFA	Trifluoridic Acid
	THF	Tetrahydrofuran

1 Introduction

1.1 Background

In recent years, nanomaterials have been a core focus of nanoscience and nanotechnology, which is an ever-growing multidisciplinary field of study attracting tremendous interest, investment and effort in the research and development around the world [1]. Nanoporous materials are also of scientific and technological importance due to their vast ability to absorb and interact with atoms, ions and molecules on their large interior surfaces and in the nanometer sized pore space. Nanoporous materials, as a subset of nanostructured materials possess unique surface, structural, and bulk properties that underline their important uses in various fields such as ion exchange, separation, catalysis, biological molecular isolation and purifications. They offer new opportunities in areas of inclusion chemistry, guest-host synthesis and molecular manipulations and reaction in the nanoscale for making nanoparticles, nanowires and other quantum nanostructures [1].

Porous materials are like music: the gaps are as important as the filled-in bits. The presence of pores (holes) in a material can render itself all sorts of useful properties that the corresponding bulk material would not have [1]. Nanoporous materials are a subset of porous materials typically having large porosities, greater than 0.4, and pore diameters less than 100 nm, giving them unique properties such as a high surface to volume ratio, high surface area, large porosity and a very ordered uniform pore structure [1].

Nanoporous materials abound in nature, both in biological systems, and in natural minerals. The walls of our cells are nanoporous membranes, although with a lot of added complexity, and the petroleum industry has been using natural nanoporous materials, zeolites, as catalysts for decades. But the recent improvements in our ability to see and manipulate on the nanoscale are beginning to allow us to design and create a wide variety of nanoporous materials as well as controlling the pores size and modifying physical and chemical characteristics of the materials used to make up the pores.

Polymeric nanoporous materials derived from block copolymers offer great technological promises due to their many potential applications as, e.g., size selectivity

separation membranes, sensors, substrates for catalysis, templates for electronic devises, and depots for controlled drug delivery. The mutual repulsion between two blocks in the copolymer, di-block copolymer, molecule provides for microsegregation on the nanometer length scale [2]. Di-block copolymer phase behavior is controlled by two factors: the overall molecular weight and the relative amounts of the different blocks of the molecule. Symmetric compositions yield lamellar types of morphology, and increasingly more asymmetric compositions gives a cylindrical or spherical morphologies [3]. The relationship between the achieved well defined structure of the block copolymers and the phase diagram is exemplified in figure 1. If one polymer block is either glassy at room temperature or crosslink able in the assembled state, and the other polymer block is removable from the matrix, it is possible to create a nanoporous material by selectively removing one polymer block from a di-block copolymer.

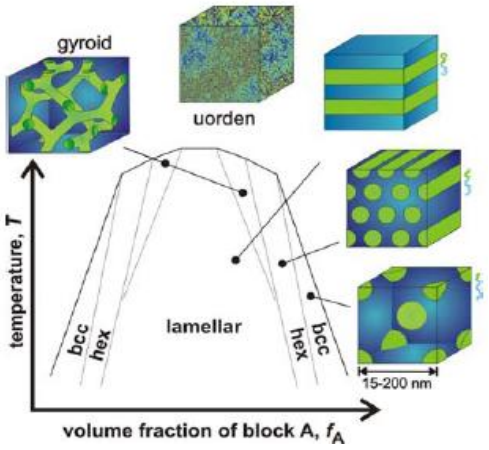

Figure 1 Phase diagram of block copolymers [3]

The technique currently used to create porous materials out of block copolymers have some disadvantages due to the time consuming method used to produce the copolymers, becoming, therefore, a very expensive process to be applied industrially. In order to meet the requirements for an industrial application a new method for creating nanoporous materials out of interpenetration networks, instead of di-block copolymers, was developed and showed promising results. The greatest benefit of this new developed method is the time and money saving process. This is achieved by using commercially

available monomers and polymers instead of block copolymers which have to be deliberately synthesized in a time and money consuming process.

An interpenetrating polymer networks (IPN) is defined as a combination of two or more polymers in network form, where at least one of which is synthesized and/or cross-linked in the immediate presence of the other [4].

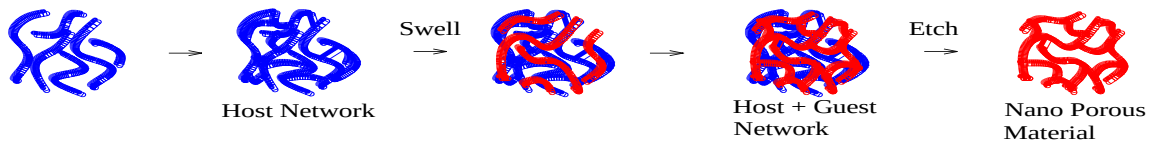

Figure 2 Scheme of nanoporous material creation

The technique used to create nanoporous polymers out of interpenetrating network can be described as the following: A polymeric network, from now on called host network, is created by cross-linking a commercial available polymer. This network is then swollen in a mixture of monomer/ initiator/ cross-linker which will polymerize and cross-link inside the host matrix, creating an IPN. Thus, the second network will be, from now on, called guest network. In order to generate a nanoporous material (NPM) out of an IPN, the host network structure has to be etched away. After the etching, the guest network is supposed to keep its structure creating a nanoporous polymer [5]. The process of creating a nanoporous material out of interpenetrating networks is exemplified in the figure 2. In order to use this method as a time and money saving process, commercially available monomers and polymers were used instead of deliberately producing block copolymers.

1.2 Problem Description

Interpenetrating networks is a promising method to create nanoporous materials in an inexpensive and uncomplicated way based on simple chemistry. In this work this new technique is used to study the influence of the cross-linking degree of the host network on the size of the nanopores.

By increasing the cross-linker degree the swelling ratio of the host network decreases. As a result, it is expected that less space is left to guest polymer to polymerize within the host network and consequently the pores would be bigger. On the other hand,

if the amount of cross linker is excessively small, is not possible to make a network out of the host network. Therefore the optimum condition has to be found.

1.3 Scope

This work is divided in four parts. Firstly a small literature review where the porous materials are introduced and the main methods of production and possible applications of the nanoporous polymers are discussed. A second part where the experimental procedure, as well as the materials and reactants used, are described. A third part where the results are presented and discussed. And finally the conclusions, together with the recommendations, are described.

2 Literature Review:

To provide a comprehensive state of arte of nanoporous materials, this chapter will begin with a brief introduction in which the pores and porous materials are defined and the main properties and characteristics are presented. This introduction is followed by a description of the main techniques used to produce nanoporous materials, and finally the major application opportunities are presented.

2.1 Definition of pores and porous materials

Pores are generally classified as open pores, which connect to the surface of the material, and closed pores which are isolated from the outside. In separation, catalysis, filtration or membranes, often penetrating open pores are required while materials with closed pores are normally used in sonic and thermal insulation, or lightweight structural applications. Pores can have various shapes and morphologies such as cylindrical spherical and gyroid, and they can be straight or curved or with many turns and twists thus having a high tortuosity [1].

International Union of Pure and Applied Chemistry (IUPAC) classifies porous materials into three categories [1] - microporous with pores of less than 2 nm in diameter, mesoporous having pores between 2 and 50 nm, and macroporous with pores greater than 50 nm. The term nanoporous material has been used for those porous materials with pore diameters of less than 100 nm and typically having large porosities, greater than 0,4. The high surface to volume ratio (high surface area and large porosity) and a very ordered, uniform pore structure make the nanoporous materials properties so unique. They have versatile and rich surface composition and properties, which can be used for functional applications such as catalysis, chromatography, and separation and sensing [1].

2.2 Properties and characterization of nanoporous materials

Nanoporous materials possess a unique set of properties that the bulk correspondent materials do not have such as high specific area, fluid permeability and molecular sieving and shape - selective effects. Different nanoporous materials with different pore size, porosity, pore size distribution and composition have different pore and surface

properties that will eventually determine their potential applications. For different applications there are different sets of performance criteria that would require different properties [1].

2.3 The nanoporous materials Production

In a study co-founded by the 6th framework program of the European Commission in 2005, [6] the different steps in the nanoporous materials production is reviewed and schematized in four important sectors: template preparation; synthesis and functionalisation. The last step is intended to provide the nanoporous material with properties required for the final application. However the nanoporous material production does not always follow this linear approach. In many cases, different applications use one or few specific templates, synthesis and functionalisation processes that lead to the desired properties whished, fulfilling other industry specific requirements such as cost, throughput and flexibility [6]. The table 1 summarizes the production techniques considered within this chapter. For each of them a brief description is given and the main problems are outlined.

Table 1 Overview of the processes reviewed by the European Commission in 2005 [6]

Template preparation	Material synthesis	Functionalisation
• Mesoporous structures; • Colloidal suspensions; • Block copolymers	• Solution precipitation; • Self-assembling; • Liquid Crystal routs; • Swelling; • Supercritical fluids; • Lithography	• Solvents for templates removal; • Etching; • Post-modification/grafting

2.3.1 Template Preparation

The production of nanoporous structures with controlled pore sizes, morphology and size distribution usually involves the use of tailored templates. Their use provides the conditions for raw materials self assembling in the desired way and is absolutely required for long range arrangement of the nanoporous materials (especially for the

mesostructure). When these templates are removed the porous material is obtained. Template preparation methods can be grouped in two main groups: substrates which pattern and / or structure is reproduced in the nanoporous material, and particles suspensions that act as precursors of the pores and around which the nanoporous material is formed [6].

This section will briefly describe the fundamentals of the three main processes used for preparing templates. However, due to the variety of nanoporous materials applications and required properties, many different template processes are being researched or customized to specific applications.

2.3.1.1 Mesoporous structures

This method consists on using nanoporous structures as templates for creating new nanoporous materials. For instance, mesoporous silica with 3-D connected pores network is used to produce non- siliceous mesoporous materials such as carbon. After that the silica framework is burned off and the carbon mesoporous material remains [6].

The main barriers for this process development, highlighted in [6], are the price, especially for bulk materials, and the lack of suitable block-copolymer templates. In fact, the use of block copolymers that provide silica materials with microporous structure seems not that suitable for non-siliceous materials because they are normally not robust enough to maintain the mesostructure upon the formation of the oxide [6].

2.3.1.2 Colloidal suspensions

This template method is mostly used for the production of bulk materials. Most widely used colloids are Silica and polystyrene latex, both commercially available. The advantage of Si colloids is that it can be dispersed in water, or ethanol, and etched by acid solutions. On the other hand, polymer latex colloids can be removed by heat or solvent treatment. Over the last years, polymer colloids are also functionalized leading to core-shell polystyrene spheres with silica onto their surface that offers the possibility to make 3-D photonic crystals with tunable optical properties [6].

According to [6], the main problems refer to the price and the availability of suitable monodisperse inorganic/organic colloidal suspensions.

2.3.1.3 Block copolymers

Block copolymers are macromolecules made up of two or more distinct blocks covalently bonded together. One way to create nano porous materials is using self-assembled di-block structures. The copolymers consist of two immiscible polymers and, due to the immiscibility, on one hand, and the chemical connections on the other, a phase separation occurs in the nano scale. Block copolymers have the ability to self- assemble into predictable highly ordered structures by means of altering process temperature; chemical composition and molecular architecture (see figure1). Moreover, block copolymers have rich structural properties and phase (separation) behavior [6]. Surfactant aggregate to micelles in a solution above their critical micelle concentration and a network enclosing the hydrophobic part of the micelle is formed. After removal of the template, pores are established with shapes according to the aggregates morphology. The resulting nanoporous materials have many potential applications including catalytic conversion, separation media, inner-layer dielectrics, and templates for the synthesis of other materials.

The preparation of nanoporous materials by the specific removal of a minority block in a block copolymer has attracted the attention of many researches and a number of more or less quantitative and specific cleaving schemes have been proposed.

2.3.2 Nanoporous material synthesis

A broad range of methods could be used for synthesizing nanoporous materials, however, few of them get most attention.

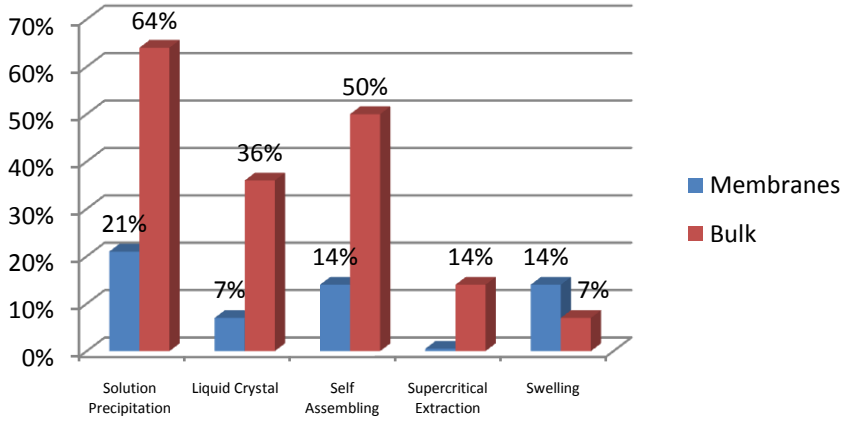

Figure 3 Typical methods used for the synthesis of nanoporous materials [6]

2.3.2.1 Sol-gel method / solution precipitation routs

In solution precipitation routs, the precursor of the nanoporous material is dissolved in the solution and precipitates due to chemical reactions (normally accelerated by means of catalysts). In the sol-gel method, the precursor is in the form of micro-sized particles (usually inorganic metal salts or organic compounds such as metal alkoxides) mixed with solvent (sol, short for solution), like water or alcohol. This solution acts as the precursor for an integrated network (or gel). When the micro-sized particles and the solvent are mixed, a suspension is formed. This process works at room temperature and consists of four main steps:

- Hydrolysis;
- Condensation and polymerization of the particle;
- Growth of particles;
- Agglomeration and formation of networks.

The outcome of the process depends on several factors that influence the hydrolysis and condensation rates. Among them, there are few that are considered to have greater impact: ph, nature and concentration of catalysts, H_2O/precursor molar ratio and temperature [6].

The sol-gel could be used to produce a wide range of materials structures such as nanoporous membranes and aerogels. Besides that, this process could be used to produce nanostructures such as thin film coatings, ceramic fibers, powders, etc.

Although the sol-gel process is considered by many as a well- established process, apart the price factor several technical obstacles have been identified, such as reproducibility of the process, purity of the nanoporous structure and difficulties in adapting the material characteristics to specific applications [6].

2.3.2.2 Self-assembling

Self assembling process is a bottom-up approach that basically consists on designing atoms and molecules that undergo a physical, chemical, or biological process that ends up with the atoms and molecules being at the right place forming the right structure. It lies on the principle that one or more of a variety of forces drive atoms and/or molecules to self organize into structures, which will be those that represent lowest energy configurations within the particular constrain of the environment [6].

The main advantages of self assembly processes are that they do not require scaling down the manufacturing tools presently required and, because they are a bottom-up approach, they require less raw material and produce less waste. The main barrier of this process is the design of complex systems.

2.3.2.3 **Liquid Crystal routes**

Liquid crystal phases, at high enough concentrations, can replicate their liquid crystalline structures, thus repeating distance and mesophase of the liquid crystal phase. This could lead to large continuous domains (in the range of mm) of mesoporous structures. That is advantageous as compared to template methods based on the cooperative assembly principle. According to the [6] there are price and technical obstacles both for membranes and bulk materials. The need for new templates also involves costly synthetic procedures.

2.3.2.4 **Swelling (for polymers)**

Swelling is the increase of volume of material, usually due to absorption of a solvent. The swelling behavior of polymer cross-linked matrices, derived from block copolymers, depends on the cross-linking degree of the blocks. For instance, the presence of double bonds in the nanoporous polymer facilitates a controlled introduction of functional groups onto the pore walls, which leads to the opportunity of controlling the internal surface characteristics of the nanoporous cavities. Several morphologies, templated from the self-assembled diblock copolymer structures, are conserved in the resulting cross-linked matrix. The main technical barrier of this process is that the pores can collapse upon solvent removal [6].

2.3.2.5 **Supercritical fluids**:

The unique physical characteristics of supercritical fluids, like CO_2, are used to produce well-defined nanostructures for potential applications in inorganic catalyst supports. Supercritical fluids minimize the surface tension and capillary forces, between the solvent and precursors, which have shown to be highly destructive at the nanoscale. Processes based on supercritical fluids offer a very good control over solvent variables such as density, dielectric constant and polarisability. Changing pressure conditions instead of temperature performs control of processes variables. This is highly

advantageous as pressure propagates much faster than temperature. However, according to the experts there are still price and technical barriers to be overcome. The possibility to avoid the use of organic solvents may make this method attractive for producing biocomposite materials [6]. This process could also be used for functionalizing the pores. The lowest viscosity of supercritical fluids allows an easier penetration into the porous structure providing a complete and more homogeneous functionalisation [6].

2.3.2.6 Lithographic approaches

Main lithographic approaches to create nanoporosity consist of bombarding a material with light, electrons or an ion beam to physically change its surface. Patterning can be achieved through the use of a mask or by direct control of the beam. The wavelength of the light being used limits the minimum achievable feature size for light to around 30 nm.

Traditional light-based lithographic processes have been widely used in several industries. Approaches using electrons, ions or atoms for bombarding the material are also being developed and some of them already applied in pilot plants [6]. These approaches do not require masks and are able to directly modify the surface. They could also lead to close to nm precision. However, they cannot create structures simultaneously, becoming very expensive. Therefore, they are presently used for creating masters for soft nanolithography or for preparing templates used in self-assembling production methods. Soft lithography / imprinting methods can be used in the creation of nanoporous materials or templates.

2.3.3 Post treatment and functionalisation

Most applications of nanoporous materials require special characteristics that cannot be achieved by means of standard processes.

There are 2 main approaches for providing the required functionality:

- Post modification (grafting method) or
- Direct synthesis (co-condensation of the functional groups).

The co-condensation method is mostly applied to the sol-gel process and basically consists on adding the functional groups to the sol so they undergo the normal production process. This process allows a high load of functional groups but has a negative impact

on the long-range order of the mesoporous structure. In addition, only limited functional groups could be applied with this method and there is also the risk of losing part of the achieved functionality during template and solvent removal. In figure 4 the most used functional methods, according to [6], are presented.

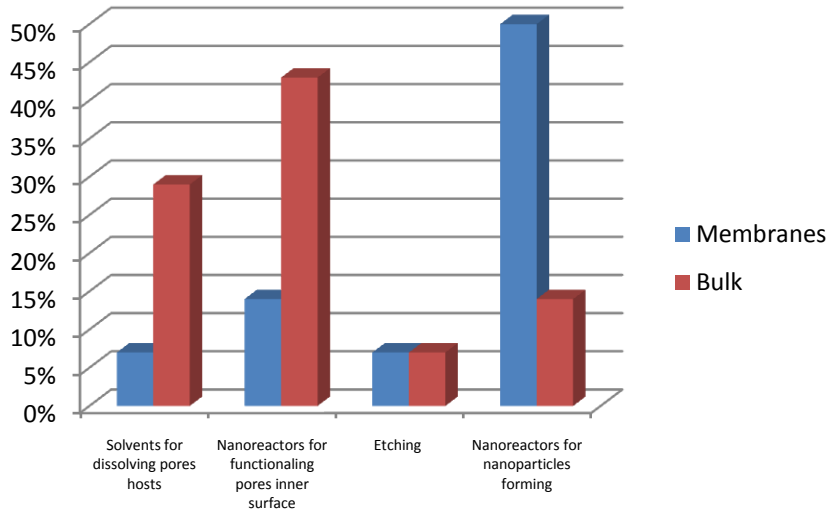

Figure 4 Typical used functionalisation methods

This section presents the post processes required for completing the production of a nanoporous material, such as solvents and precursors removal.

2.3.3.1 Solvents for dissolving pores hosts/precursors

Many nanoporous production methods make use of templates or structure directing agents (SDAs) to achieve the required nanoporous material. Once the material has grown the pores precursors remain inside and need to be removed for achieving the final porous structure [6].

The use of solvents for dissolving the precursor is widely used but has an important drawback: in many cases the SDAs are destroyed during the process. These SDAs are tailored to the specific shapes and morphology and therefore are normally very expensive. Also the process undergone to eliminate the pores precursors, like high temperature processes, may endanger the resulting nanoporous structure. This procedure also has a negative environmental impact.

2.3.3.2 Etching

The nanoporous material can be obtained either by passing an electric current through the semiconductor (dry etching) or by being in contact with a strong acid solution (wet etching). When both etching processes are combined the acid reacts with the material leaving behind a sponge-like structure that is full of linked pores and the current controls the fraction of the material that dissolves where the front of acid has reached. Therefore is possible to vary the porosity form place to place by changing the current as the etching progresses. Thus is easy to produce multi-layered structures, with different pores size and refractive index. The main barrier to be overcome is the need of experimental equipment for programmed etching.

2.3.3.3 Post – Modification / grafing

The so-called grafting method allows the functionalisation of the surface of the pores with various chemical functionalities, both organic and inorganic, even maintaining the mesostructure after the functionalisation. However, the density of functional groups to be added is limited and not uniform due to the constraints for accessing the pores. Moreover, this type of functionalisation reduces the surface area and the volume of the pores.

In open nanoporous materials, pores are part of an interconnected network in which connections are normally smaller in diameter than the pores they connect. Therefore, the only way to get the functionalizing substances in the nanoporous interconnections is to separately feed the different components of the functional molecule and make them react inside the pore, which is acting as a chemical reactor of nanometer size. Stability is one of the main requirements for nanoporous materials and therefore is one of the requirements to be fulfilled after the functionalisation has been completed [6].

2.4 Major opportunities of application

There are ever expanding applications for nanoporous materials besides the traditional areas of adsorption separation, catalysis and membranes. This section intends to give an overview of the main application opportunities and market potentials.

2.4.1 Environmental separations

As the regulatory limits on environmental emissions become more and more stringent, industries have become more active in developing separation technologies able to remove contaminants and pollutants from waste gas and water streams.

Adsorption process and membranes separations are two dominating technologies that have attracted continuous investments. Adsorbent materials and membranes (typically nanoporous) are increasingly being applied and new adsorbents and membranes are constantly being invented and modified for various environmental applications such as the removal of SO_2, NO_x and VOCs emissions [7].

New adsorbent materials with well defined pore sizes and high surface areas are being developed and tested for potential use in energy storage and environmental separation technologies. Table 2 lists some examples of new adsorbents for energy and environmental applications as identified by Yang [8]

Table 2 Examples of emerging process for environmental separations [8]

Energy and Environmental Applications	Adsorbents and Technology
CH_4 storage for on-board vehicular storage	Super – activated carbon and activated carbon fibers; Near or meeting DOE target storage capacity
H_2 storage for on-board vehicular storage	Carbon nanotubes possible candidate
N_2/CH_4 separation for natural gas upgrading	Clinoptilolite, Sr-ETS-4 by kinetic separation
Sulfur removal from transportation fuels (gasoline, diesel and jet fuels)	π-complexation sorbents such as Cu(I)Y, AgY
CO removal from H_2 to < 10 ppm for fuel cell applications	π-complexation sorbents such as CuCl/y-Al_2O_3, CuY and AgY; silica molecules sieve membranes
NO_x removal	Fe-Mn-Ti oxides; Fe-Mn-Zr oxides; Cu-Mn oxides
Removal of dienes from olefins (to <1 ppm)	π-complexation sorbents such as Cu(I)Y, AgY

2.4.2 Clean Energy production and storage

Future energy supply is dependent on hydrogen as a clean energy carrier. Hydrogen can be produced from fossil fuels, water electrolysis and biomass. However, the current debates on the hydrogen economy are intimately linked to the clean production of hydrogen from fossil fuels such as natural gas and coal. Due to the low cost and wide availability of coal, coal gasification to syngas and then to hydrogen through the water gas shift reaction is a promising rout to cheap hydrogen. The success of such a hydrogen production rout will be only possible if carbon dioxide is sequestered safely and economically. The key to the cost effective conversion of coal to hydrogen and carbon capture is nanomaterials development such as catalyst for the water-gas shift (WGS) reaction and inorganic membranes for hydrogen/CO_2 separations [1].

In the future hydrogen will be the dominant fuel, and converted into electricity in fuel cells, leaving only water as a product. Fuel cell development has been very rapid in recent years. However, there are many technological challenges before fuel cells become commercially viable and widely adopted. Many of the problems are associated with materials notably related to electrocatalyst, ion-conducting membranes and porous supports for catalyst. Certain nanoporous materials, such as carbon nanotubes and zirconium phosphates, have already shown promise for application in fuel cells [1].

Hydrogen storage will also be essential. It can be stored in gaseous, liquid and more recently in solid form. Nanostructured materials, such as carbon nanotubes, show promising results as an adsorbent. Despite many controversial reports in the literature, hydrogen storage in carbon nanotubes may one day become competitive and useful [1]. Another type of nanostructured carbons is templated by using 3-D ordered mesoporous silicates. It has been shown that this type of carbons exhibit interesting and superior performance as supercapacitor and electrode materials for Li –ion battery applications [9].

2.4.3 Catalysis and photocatalysis

Heterogeneous catalysis has a major impact on chemical and fuel production, environmental protection and remediation and processing of consumer products and advanced materials [1]. More efficient catalytic processes require improvement in catalytic activity and selectivity. Both aspects will reply on the tailor- design of catalytic

materials with desired microstructure and active site dispersion. Nanoporous materials offer such possibilities in this regard with controlled large and accessible surface area of catalyst but avoiding standalone fine particles. The traditional methods of impregnation of metal ions in nanoporous supports are not as effective in achieving high dispersion of active centers, whereas incorporation in templates synthesis or intercalation are more advanced techniques rendering high activity owing high surface area of the active components and selectivity due to the narrow pore size distribution [1].

2.4.4 Sensors and actuators

Nanoparticles and nanoporous materials possess large specific surface areas, and high sensitivity to slight changes in environments such as temperature, humidity, and light. Therefore such materials are widely used as sensor and actuator materials. Gas sensors reply on the detection of electric resistivity change upon change in gas concentration and their sensitivity is normally dependent on the surface area. Gas sensors based on nanoporous metal oxides such as SnO_2, TiO_2, ZrO_2 and ZnO are being developed and applied in detectors of combustible gases, humidity, ethanol and hydrocarbons. Zirconia is typically a good sensor material for oxygen [1].

2.4.5 Biological application

Nanomaterials that are assembled and structured on the nanometer scale are attractive for biotechnology applications since the potential to use material topography and the spatial distribution of functional groups to control proteins, cells, and tissue interactions, and also for bioseparations. Bionanotechnology creates materials, or biomaterials, for biological applications [1].Many studies are an underway in fundamental understanding and exploiting the nature of nanoscale systems and processes to:

- Develop improved chemical separations and isolation media using nanoporous materials;
- Integrate engineered and self-assembled materials into useful devises ranging from biosensors to drug delivery systems;

- Developed new products and biomedical devices by manipulating biomolecules enzymes, other proteins, and biochemical processes at the nanoscale.

Proteins have been used by nature for billions of years to create complex structures within a living cell. They provide superior catalytic abilities over traditional inorganic type catalysts and the simplified reaction conditions of enzymes require less complex engineering than catalytic reactors. Nanoporous materials, being porous and some often found bio-compatible, afford the capability to build enzymatic nanomaterials that mimic natural biological reactions. Immobilizing recombinant enzymes into nanoporous materials can be used for long-lifetime biological reactors for a variety of applications. The possibilities for using enzymes in small-scale reactors for producing drugs, energy, decontaminating wastes, and creating complicated synthetic reactions are limitless [13].

Nanopores embedded in an insulating membrane fabricated by using a physical method has been demonstrated useful to examine biomolecules one by one, achieving single-molecule analysis [1]. On the other hand an ion beam can also be used to shrink pores of micrometer size, in a silicon nitride membrane, down to nanoscale dimensions for measuring the motion of single DNA molecules through the nanopores [1]. The most overseen result of the work is that the DNA molecules do not thread meekly through these nanopores like a noodle of spaghetti, but instead comes through the pores in several configurations. This is an important breakthrough towards DNA sequencing, demonstrating the potential applications of nanoporous materials in bioengineering [1].

Another interesting area of applications as far as nanoporous materials are concerned is biosensors. Piezoelectric biosensors using high surface area nanoporous coatings exhibit increased sensitivity in detection. Immobilized biological molecules on the surface of nanoporous silica can provide as biological detection systems [1], microscale piezoelectric cantilevers serve as the transducer. There is a shift in resonance frequency of the cantilever when molecules adsorb onto its surface. The shift in frequency results from the change in mass of the adsorbed analyte to the mass of the cantilever [1]. Biosensors have major potential in the healthcare industry, where, for example, real-time in vivo sensing could be used for insulin pumps, drug detection in

emergency situations. Rapid methods for detecting pathogens in food products and animal feed could save billions of dollars in medical costs [1].

2.4.6 Other applications

Besides the above applications, there are also tremendous opportunities for nanoporous materials in the following areas [1]:

- High efficiency filtration and separation membranes;
- Catalytic membranes for chemical processes
- Porous electrodes for fuel cells
- High efficiency thermal insulators
- Electrode material for batteries
- Porous electronic substrates for high speed electronics.

2.5 The groups knowledge

The present work is a lateral investigation made in the Nanogroup. This group was born from a partnership between the Danish Technical University and the Danish National Laboratory in Risø dedicated to investigate the creation of highly ordered polymeric nanoporous materials for several applications. The nanoporous materials that are produced within this group are mainly created from Polydimethylsiloxane (PDMS) containing block copolymers. The other part of the block copolymer is either polysterene (PS), polymethylmethacrylate (PMMA) or polyisoprene (PI). The block copolymers are readily synthesized by living anionic polymerization and the block copolymer precursor is aligned in a shear field. Some schematic examples of the types of nanoporous polymers realized are shown in the illustration below: the white regions represent the voids in a polymer matrix (blue).

Figure 5 Examples of the types of nanoporous polymers realized by the Nanoporous Group

These materials are obtained from the selective degradation of one part of the diblock molecules. PDMS is quantitatively mainly etched in two ways: Anydrous hydrogen fluoride (HF) or tetrabutylammonium-fluoride (TBAF).The scheme for HF allows the preparation of unlinked glassy nano-porous structures, and also makes it possible to make bulk materials of spherical cavities. Etching with TBAF requires the presence of a solvent, thus this is only possible in cross-linked samples [3]. The only disadvantage of this technique is that the copolymers need to be deliberately produced, consuming, therefore, a lot of time and becoming too expensive to be applied industrially. To meet the requirements for an industrial application, a research began, last year, as a parallel investigation where a study about the creation of nano-porous materials out of commercially available substances, Polydimethylsiloxane (PDMS) and Polymethylmethacrylate (PMMA), in an economic process was made and a procedure based in interpenetrating networks was developed [5]. This report, using the same procedure developed in the previous study to produce NPM, aims to study the influence of the cross-linking degree of one of the networks in the size of the pores, of the final nanoporous materials.

2.5.1 Preparation of PDMS-PMMA Interpenetrating networks

In the present study, has previously referred, nanoporous materials are created from PDMS-PMMA interpenetrating networks. Interpenetrating polymer networks (IPNs) are defined as combinations of two or more polymers in network form, with at least one of the polymers being polymerized and/or crosslinked in the immediate presence of the other(s) [4]. The most reported technique for the preparation of PDMS-PMMA interpenetration networks is the monomer immersion method. This method is characterized by the immersion of a cross-linked PDMS sample in a mixture of MMA/initiator/cross linker for 18 hours at room temperature. The most commonly used initiator is a 2,2 – dimethoxyacetophenone, a UV- sensitive free radical initiator, and the mostly used cross-linker is triethylene glycol dimethacrylate (TEGDMA). The swollen PDMS (pre-IPN film) is then washed and immersed in MMA monomer, without cross-linking agent or photo initiator and placed under a UV light of 32 W and a wavelength of 350 nm for 1 hour [10][11][12].

3 Experimental Part

In this chapter the methodology used to produce nanoporous material out of IPN is presented. This technique can be divided in 3 main stages [5]:

1. Creation of host network;
2. Creation of IPN by swelling the host network in a mixture of polymer/ Initiator/ Cross-linker, followed by the formation of the guest network within the host matrix;
3. Creation of the Nanoporous material by etching the host polymer network.

In order to study the influence of cross linking degree in the size and morphology of the pores, three samples with different amounts of cross-linker were prepared. Further on, the sample nomenclature is written as **X_%** where X is the kind of sample (PDMS film, IPN or NPM) and % is the molar percentage of PDMS cross-linker, DCP, calculated by the following equation:

$$DCP\ mol\% = \frac{n(DCP)}{n(active\ \ chain)} \times 100 \qquad (3.1)$$

where the active chain is the polymeric chain between two successive cross links.

3.1 Existing networks

Polydimethylsiloxane (PDMS) shows several interesting properties such as low surface area, high permeability to many gases and biocompatibility [15]. On the other hand there is much experience within the Nanogroup in the synthesis and etching of PDMS networks. This is why an easier way to create an IPN would be to use a PDMS network together with another polymer. The idea is to create an IPN based on a stable PDMS network. This network should then be swollen with a solution containing monomer, initiator and cross linker which is polymerized and crosslinked within the PDMS matrix. After the etching of the PDMS network, a porous material should remain.

A suitable polymer for this purpose is Polymethylmethacrylate (PMMA) [16]. This polymer is glassy at room temperature and easy to process. Besides it can be cross linked by multifunctional Methacrylates. Polystyrene (PS) is also a suitable polymer to be

combined with the PDMS network. It is glassy at room temperature and can be cross linked easily with bifunctional monomers. But, unlike the methylmethacrylate (MMA), it is cancerous, which is the main reason why MMA was chosen for further experiments.

The combination of PDMS and PMMA is already used to create more stable PDMS membranes [17]. The main focus of the work done so far was on using PDMS as the major component. It is known that it is possible to create stable IPNs with PMMA as the major component but there is not a lot of experience with such films [8].

3.2 Creation of host PDMS Networks

3.2.1 Free radical cross linking

A methylhidro-dimethyl-siloxane copolymer from Huls America Inc. was used. According to the manufacturer the copolymer has 3-4% methyl-hydro-siloxane groups. Previously, a characterization with conventional Gel Permeation Chromatography (GPC) was done giving the following results:

$$M_n=7620;\ M_w=16100;\ PDI=2{,}113.$$

Where M_n is the number average molecular weight and M_w the weight average molecular weight.

From a previous study using Fourier Transformation Infrared (FTIR) measurements [5], was proven that the polymer chains are methyl terminated.

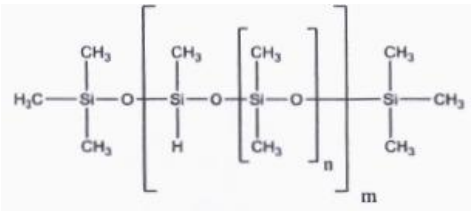

Figure 6 Structure of the Methylhydro-Dimethyl-Siloxane copolymer; n/m≈30 [5]

The polymer was cross linked by radical reaction. Dicumylperoxide (DCP) served as free radical source. On the basis of the radical cross linking scheme of [19] the following theoretical cross linking scheme was developed and proved, in a previous study, to be coherent.

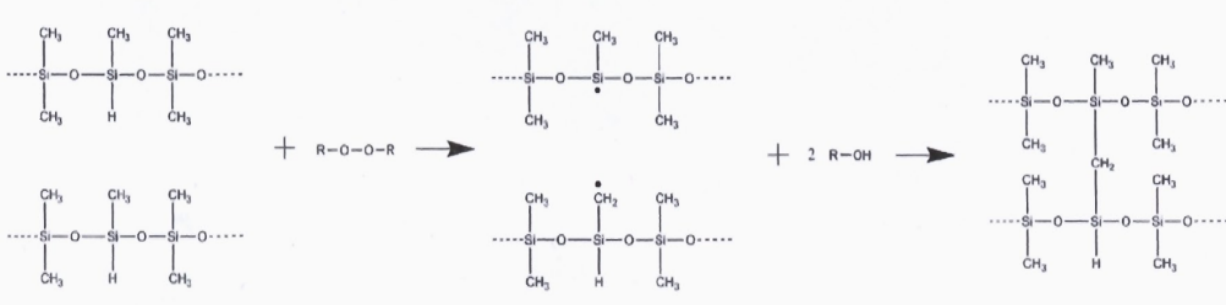

Figure 7 Reaction scheme of the radical cross linking [5]

This method was chosen for the creation of the PDMS films because the cross linking degree can be easily adjusted by varying the percentage of the free radical source.

3.2.2 Production steps

The PDMS films were prepared with the solvent casting technique, described below. Therefore the required mass of polymer was calculated over the diameter of the Petri dish, *d*, the desired thickness, *t*, and the volumetric mass of the polymer, ρ, as the following expression indicates:

$$m = \frac{\pi}{4} d^2 \times t \times \rho \qquad (3.2)$$

The amount of polymer was weighted and placed in the Petri dish. Then, the needed amount of cross-linker was calculated as a molar percentage of the polymer, weighted and placed in a beaker. In order to ensure a good distribution of the DCP in the polymer, the technique of solvent casting was applied: The DCP was dissolved in THF and the solution was poured into the Petri dish. The mixture was left overnight to evaporate slowly under a slight flow of nitrogen at room temperature.

After evaporating the entire solvent the Petri dish was placed in a sealable metal cylinder to prevent volatile substances from evaporating during the cross-linking process. The metal cylinder was flushed with nitrogen in order to prevent the polymer from oxygen and other reactive gases during the cross-linking process. Then, the cylinder was placed in a 140 °C preheated laboratory oven for two hours. After being cooled down, the Petri dish with the cross linked PDMS film could be removed.

Figure 9 Petri dish inside the metal cylinder (9 cm inner and 10 cm outer diameter)

Figure 8 Metal cylinder being flushed (9 cm inner and 10 cm outer diameter)

In order to study the influence of the cross linking degree of the PDMS network in the size of the porous, 3 samples with different amounts of cross-linker were prepared in the same conditions (ex: 40 mol%, 60 mol% and 75 mol %). The properties of the samples are presented in table 3.

Table 3 Properties of the PDMS samples

Sample	$d_{Petri\ dish}$ / [cm]	t / [cm]	$\rho_{polymer}$ / [g/cm3]	$w_{polymer}$ / [g]	w_{DCP} / [g]	mol %DCP
PDMS_40				3,458	0,218	40,06
PDMS_60	5,5	0,15	0,970	3,453	0,327	60,09
PDMS_75				3,500	0,409	74,24

PDMS networks are transparent and rubberlike. By handling the samples it became obvious that increasing the cross-linking amount, the samples appear more fragile, sticky, and braking more easily into little pieces when removed from the Petri dish.

3.3 IPN creation

Interpenetrating polymer networks are combinations of crosslinked polymers held together by permanent entanglements [12].PMMA was chosen as a collaborating polymer

because the glass transition temperature lies above 100 °C and it is a transparent polymer in the glassy state. PMMA is also cheap, easily available and non-poisonous. This polymer can be polymerized by free radical polymerization and therefore be combined with various vinyl based monomers. Moreover MMA showed good swelling properties for the PDMS films.

The initiator that combines all the required properties was azobisiobutyronitrile (AIBN). It has a high decomposition rate at temperatures above 25 °C.

In order to create a real interpenetration network, the PMMA polymer has to be cross-linked. The solvent used in the etching process (THF) make the cross-linking necessary, preventing the PMMA from being solved and the formed structure from being destroyed when the PDMS matrix is removed [5]. To obtain a cross linked PMMA matrix multifunctional methacrylates are blended with the monomer. These so called cross linkers have two or more functional groups which take part in the radical polymerization. They are able either link two polymer chains together or to start the growth of a further polymer chain at their second functional group. The cross-linking degree depends on the fraction of cross linker mixed with the monomer.

In this study, the bifunctional methacrylate used to cross link the PMMA was Diethyleneglycoldimethacrylate (DEGMA).

3.3.1 Procedure for the swelling of the host network

A sharp instrument was used to cut samples out of the PDMS films. These samples were weighted and swollen in the monomer/cross-linker/initiator mixture for one hour under a gentile agitation at room temperature.

In order to study the effect of cross linker degree, the added mixture composition was the same in all samples. Due to a previous research, the amounts of initiator and cross linker were chosen to be 1,2 wt% and 6,2 mol%, respectively [5]. The amounts used in each sample can be seen in the following table:

Table 4 Properties of the IPN samples

Sample	Mass of MMA	Mass of initiator	wt% initiator	Mass of Cross Linker	mol % of cross linker
IPN_40	3,018	0,043	1,21	0,452	6,22
IPN_60	3,015	0,042	1,20	0,447	6,15
IPN_75	3,021	0,042	1,20	0,453	6,24

3.3.2 Formation of the Guest network - Petri Dish Sandwich Method

For the polymerization of the MMA inside the PDMS network a Petri Dish Sandwich Method was used (see figure 5). In this technique the polymerization is carried out between two Petri dishes.

Firstly the swollen film is placed in a Petri dish and doused by a mixture of monomer (70 wt%) and initiator, until the film is fully covered by the liquid. On top of the film a slightly smaller Petri dish prevents the mixture to evaporating.

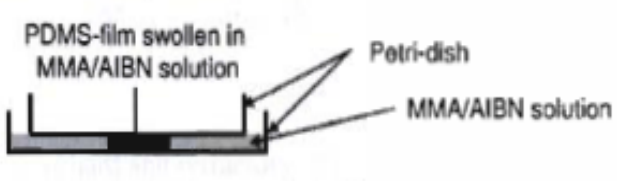

Figure 10 Scheme of the Petri Dish Sandwich Method [5]

Like was done previously for the cross-linking of the PDMS film, the construction was placed in the metal cylinder, exposed to nitrogen and placed in a pre-heated laboratory oven. The polymerization was done for 2 hours at 80°C. After the cylinder cooled down, the samples were removed.

Observing the IPN samples created is clear that the sample with 40 mol% of DCP present opaque white and shimmering characteristic. But with the increasing amount of cross-linker degree the IPN becomes more inhomogeneous and the borders seem more transparent. Owning to its very low surface energy, PDMS is among the most incompatible polymers, so that transparency is not expected for IPNs based on PDMS. However, it is known that by selecting adequate synthesis parameters, highly transparent materials may also be obtained [15]. On the other hand, the more transparent is a sample, smaller is the scattering domain, and thus smaller are the pores. This fact may indicate, in

a primary stage that by increasing the PDMS cross linker the resulting pores of the NPM should be smaller.

3.4 Etching

Etching is the procedure that involves the selective degradation of one network of the interpenetration network. In this case it is used to eliminate PDMS network from the IPN films. During the reaction, fluoride ions are used to cleave the Si-O bonds of the PDMS [3].

Different chemicals can be used to insert fluoride ions in the film, as presented in table 5:

Table 5 Overview of the etching agents

Name	Phase	Solvent	Reaction time
Hydrogen Fluoride (HF)	Gaseous	-	
Trifluoridic Acid (TFA)	Liquid	-	36 hours
Tetrabutylammonium Fluoride (TBAF)	Solution	THF	36 hours

Hydrogenfluoride (HF) is very dangerous for the health and was thereby not used. The big advantage of the HF is that it is gaseous and a very small molecule. Therefore it is able to etch materials that cannot be penetrated by a liquid.

TFA is also used in the group and a slightly more reactive etching more reactive etching agent than TBAF. Previous experiments with TFA were not successful because the TFA destroyed the structure of the PMMA film. That is the reason why TFA was not used as etching agent.

The preferred etching agent is the TBAF because it is the most easy one to handle and to process and it does not affect the health as the others. Another advantage is that the behavior and the handling of TBAF as etching agent are, due to a great experience, well known in the group.

3.4.1 Etching of the PDMS films

After the polymerization of the IPN films one part of the polymerized film was used for the etching. The whole film is never used, because an unetched sample is needed for the characterization to compare it with the etched part.

Initially the sample used to etch was weighted and placed in a glass beaker where was covered with the etching agent (TBAF). To prevent the evaporation of the THF present in TBAF solution the beakers were covered with a cap. The reaction needs 36 hours to be complete, but the etching procedure was stopped after 48 hours. During the etching the PDMS chains are cut into small pieces but these pieces are still in the PMMA network. To eliminate the PDMS residues in the network, the remaining PMMA matrix needs to be washed. The THF in the TBAF solution is used to wash out the PDMS chain fragments and side products of the etching. So the first washing step is pure THF to get rid of all the rests. Because THF is swelling the film, the amount of THF is reduced slowly to prevent high stress on the film during the shrinking [2]. The washing itself is processed in the steps mentioned in the table 6. Depending on the sample size a total volume of 4 to 6 ml was used.

Table 6 Steps of washing procedure

THF (vol %)	THF (V_{total}=3 ml)	Methanol (vol %)	Methanol (V_{total}=3 ml)
100	3	0	0
80	2,4	20	0,6
60	1,8	40	1,2
40	1,2	60	1,8
20	0,6	80	2,4
0	0	100	3

After the washing the samples were dried for at least 12 hours before the weight measurement and the FTIR scanning of the etched sample.

After etching the PDMS, the samples become whiter, opaque and more brittle. Even the most transparent parts of the sample, even continuing to be transparent, become less shiny.

4 Results and Discussion

4.1 Gravimetric Measurements

4.1.1 Characterization of the host network (PDMS films)

The relationship between the cross-linking degree and the swelling ratio was identified by gravimetric measurements. Cyclohexane was used as the swelling agent. Dry samples were placed in glass vials containing cyclohexane and kept under gentle stirring at room temperature. After being submerged overnight, to make sure that the swelling procedure would reach the equilibrium, a fine tissue was used to dry the sample surfaces and its mass measured. The comparison between the mass before and after the swelling gives us the swelling ratio, and can be observed in the table bellow.

Table 7 Gravimetric measurements of the swelling

Sample	mol% DCP	w_{before} /g	w_{after} /g	Ratio (w_{after}/w_{before})
PDMS_40	40,06	0,1028	0,494	4,805
PDMS_60	60,09	0,1007	0,364	3,615
PDMS_75	74,24	0,1037	0,35	3,375

As it was expected, the increasing of the amount of cross linker makes the swelling ratio decrease. This occurs because the higher the cross linker degree is, the more rigid the network becomes offering more resistance to the swelling.

4.1.2 Gravimetric analysis of the IPN samples

To create the interpenetration networks, the PDMS samples were swollen in a mixture of monomer initiator and cross linker for one hour at room temperature. Subsequently, the polymerization of that mixture within the PDMS sample was done in a pre-heated oven at 80 ºC for two hours.

Gravimetric measurements were done before and after the interpenetration network formation in order to allow the determination of the final IPN composition.

Unlike it was expected all the samples have approximately the same weight percentage of PDMS and, consequently, of PMMA. Thus it appears that the cross-linking degree does not affect on the mass composition of the IPN samples. This behavior was

not expected since the higher the cross-linking degree the lesser is the PDMS film ability to swell, as seen in table 7.

Table 8 Gravimetric measurements of IPN samples

				IPN Sample composition	
Mol % DCP	**$w_{PDMS\ film}$/ [g]**	**w_{IPN}/ [g]**	**$w_{IPN}/w_{PDMS\ film}$**	**w % (PDMS)**	**w % (PMMA)**
40	1,084	2,787	2,571	38,890	61,110
60	0,272	0,772	2,841	35,202	64,798
75	0,588	1,630	2,772	36,079	63,921

Analyzing the ratio between the weight of the IPN samples and the weight of the PDMS films, unlike it was expected and shown in table 7, the increase of the cross-linking degree does not decrease the swelling ratio. This fact suggests that either the swelling equilibrium was not achieved or that the PDMS network has a different behavior when is in contact with different components. For subsequent studies the swelling time of the PDMS sample in the monomer/initiator/cross linker mixture should be increased. Comparing to the monomer immersion method reported in several studies, in which the swelling time is 18 hours at room temperature, the time given to the PDMS to swell the monomer/initiator/cross-linker mixture is probably not enough. On the other hand, for a better understanding of the IPN formation behavior the gravimetric analysis should be done with methacrylates instead of cyclohexane, in order to insure a greater control on the process.

4.1.3 Gravimetric measurements of the samples before and after being Etched

In order to determine the percentage of the weight loss after the etching procedure, gravimetric analyses were done before and after etching and washing the samples and compared with the percentage of PDMS present in the IPN sample.

Table 9 Gravimetric measurements of the samples before (B.E.) and after being etched (A.E.)

Amount of DCP	**$w_{before\ etch}$/g**	**$w_{after\ etching}$/g**	**Weight loss (w_{before}-w_{after})**	**Weight loss %**	**w_{PDMS} % (B. E.)**	**w_{PDMS} % (A. E.)**
40 mol%	0,578	0,449	0,130	22,445	38,890	16,445
60 mol%	0,300	0,240	0,060	19,980	35,202	15,222
75 mol%	0,512	0,386	0,126	24,600	36,079	11,479

In a successful etching process, the percentage of weight loss and the PDMS mass percentage of the IPN sample before being etched should be the same. Comparing these two parameters in table 9 one can conclude that the etching procedure was not completely done since the percentage of weight loss is smaller than the percentage of PDMS present in the sample before being etched. Furthermore the weight loss does not seem to be affected by the cross linking degree of the host network. On the other hand, the PDMS weight percentage of the sample after being etched decreases with the increase of the cross-linking degree.

4.2 Methanol uptake

Since the cross-linked PMMA is neither solvable nor swell able in methanol, a basic method to get a statement about the porosity of a material is to measure the methanol uptake, since it can be assumed that the mass difference is caused by methanol that is located in the pores. Therefore, dry samples of the porous materials were weighted and immersed in methanol for two hours. After this time the samples were weighted and the masses were compared. The methanol uptake and the volume of PDMS removed in 1g of sample were calculated as followed, assuming that no PMMA was washed out:

$$\frac{v_{PDMS\ removed}}{1g\ of\ etched\ sample} = \frac{w_{before\ etching} - w_{after\ etching}}{w_{after\ etching} \times \rho_{PDMS}} \quad (4.1)$$

$$\frac{v_{Methanol\ uptake}}{1g\ of\ etched\ sample} = \frac{w_{after\ sweling} - w_{before\ swelling}}{w_{before\ swelling} \times \rho_{methanol}} \quad (4.2)$$

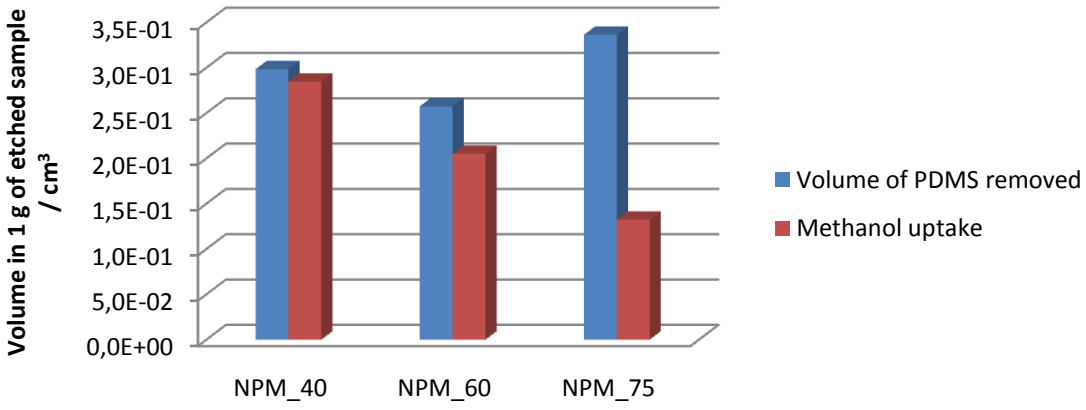

Figure 11Comparison of methanol uptake and the volume of the removed PDMS

The figure 11 shows that the methanol uptake decreases with the increase of the PDMS cross-link. This fact suggests that with the increase of the cross-linking degree, the pores are smaller decreasing the methanol uptake. On the other hand a linear relationship between the cross-linking degree and the volume of PDMS removed was expected, but no conclusion can be taken.

Ideally the methanol uptake should be equal to the volume of PDMS removed. Contrasting with what was expected, the methanol uptake is smaller in all the samples analyzed. This result may be due to the fact that the time used to the perform methanol uptake was not enough to reach the swelling equilibrium. The NPM_40 shows more promising results. Following test should have this fact in account and the samples should be in contact with methanol, for, at least 12 hours, and should be done using molar percentages of DCP around 40 mol%.. Another explanation can be due the sample morphology. Is possible that the PMMA is not sufficiently cross-linked resulting on the collapse of some pores, blocking the methanol uptake in some regions.

4.3 FTIR

FT-IR stands for Fourier Transform InfraRed, the preferred method of infrared spectroscopy. In infrared spectroscopy, IR radiation is passed through a sample. Some of this radiation is absorbed by the sample and some of it is passed through (transmitted). The resulting spectrum represents the molecular absorption and transmission, creating a molecular fingerprint of the sample with absorption peaks which correspond to the frequencies of vibrations between the bonds of the atoms making up the material. Because each different material is a unique combination of atoms, no two compounds produce the exact same infrared spectrum. Therefore, this method can result in a positive identification (qualitative analysis) of every different kind of material. In addition, the size of the peaks in the spectrum is a direct indication of the amount of material present [20].

For the measurements, a Perkin Elmer Spectrum One FTIR Spectrometer was used.

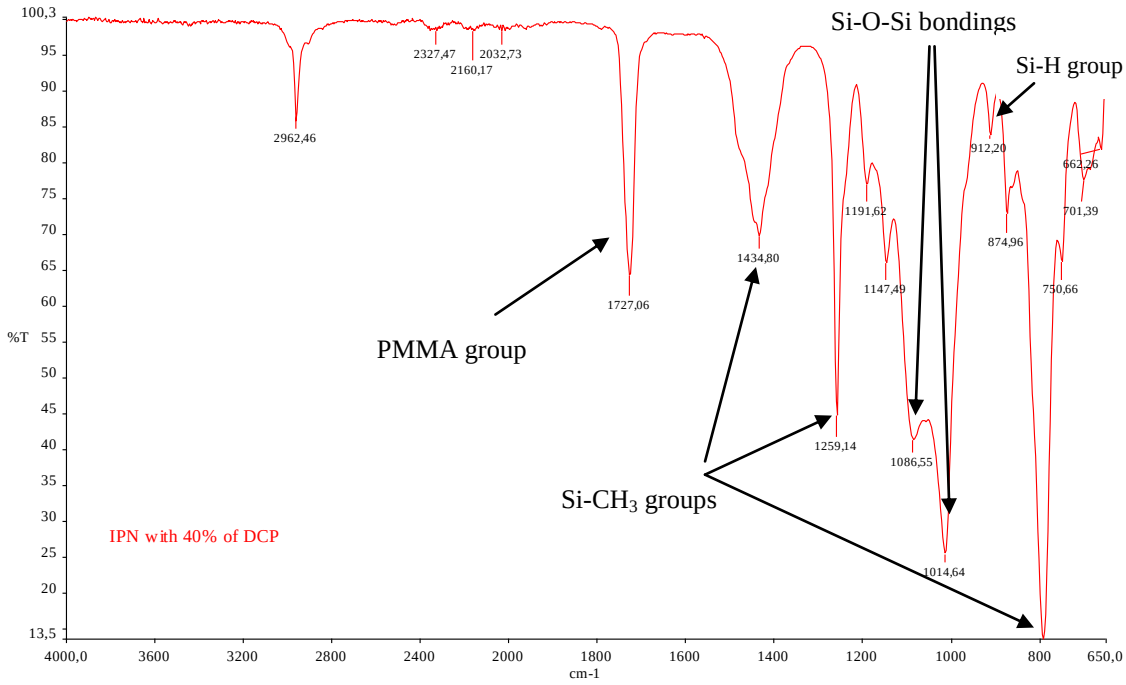

Figure 12 Example of FTIR spectrum with all important peaks – Sample IPN_40

The PDMS related peaks are the Si-O peaks between 1100 and 1000 cm^{-1} (strong) and the $Si-CH_3$ peaks at 1440 to 1400 cm^{-1} (week), 1290 to 1250 cm^{-1} (strong) and 780 to 850 cm^{-1} (strong) [21]. The decreasing of Si-O peak is a measure of etching success. The PMMA peak normally occurs between 1715 and 1780 cm^{-1} as a strong peak. All the important peaks in this study can be seen in the figure 15.

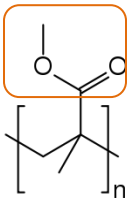

Figure 13 Functional group of PMMA that occurs in the FTIR spectrum

The quality of the recorded spectra depends on several factors. The crystal has to be cleaned with ethanol before every measurement to exclude that a small rest of the last sample is also analyzed. The film has to be flexible enough to make good contact to the crystal to ensure a good quality of the spectra. Cracks and structural irregularities can reduce the quality of the spectra which results in lower intensities and more noise [21].

4.3.1 FTIR measurements of the PDMS films

The spectrum in figure 14 shows the FTIR measurements of the polymer before and after being cross-linked with 40 mol % of DCP.

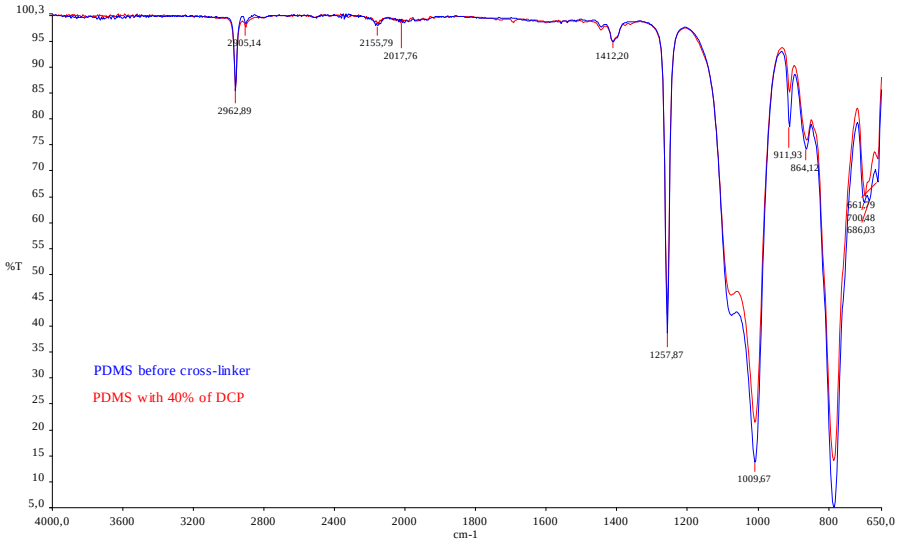

Figure 14 FTIR measurements of the PDMS before and after being cross-linked with 40 mol% of DCP

In the figure 15 the characteristic peak of the group Si-H is emphasized. As it was expected from the cross linking reaction, described in figure 7, the Si-H bounds decrease when the polymer is crosslinked.

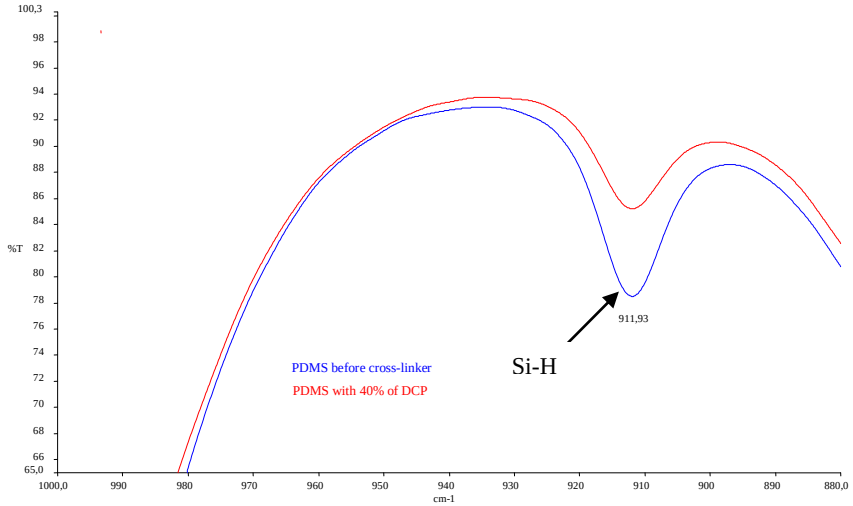

Figure 15 Detail of the peak 911,93 cm^{-1} - Si-H group

By changing the amount of DCP, on the PDMS samples, it is showed that the different spectrums have the same behavior and no significant difference is registered

(see figure 16). The decrease of the peak Si-O between 1100 and 1000 cm^{-1}, in the sample PDMS_40 may be a result of a worst quality of the spectrum.

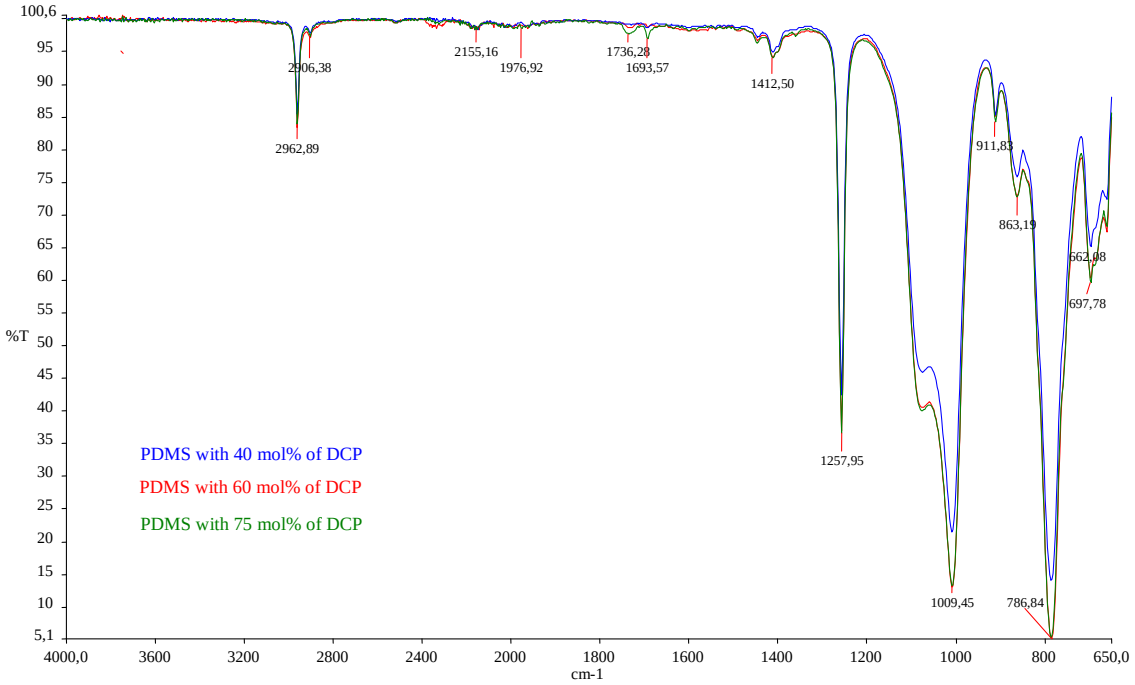

Figure 16 Effect of the different amounts of cross-linker in the PDMS films spectra

4.3.1.1 Cross-linking

In this section, a parameter to evaluate the success of the cross-linking procedure was determined and calculated from the FT-IR spectrums by comparing the intensity of a peak before and after being cross-linked. Both peaks were normalized by the peak 1256,06 cm-1, considered standard since it is characteristic of the Si-CH_3 group, thus no difference could be seen before and after the cross-linking. The peak chosen to be analyzed was the 911,38 cm^{-1}, characteristic of the Si-H group. The cross linking success is the ratio between the normalized intensity peak of the sample before being cross-linked and after being cross-linked. The calculations evolved are presented in appendix B.

As one can see from the table 10, all the samples show a successful cross-linking procedure, being the sample NPM_40 the most successful one. However no relation can be concluded between the cross-linking degree and success.

Table 10 Cross-linking success

Amount of DCP	X-linking Success (%)
40 mol %	96,46
60 mol %	83,03
75 mol %	89,08

4.3.2 FTIR measurements of the IPN films

By polymerizing MMA within the PDMS network, as it is expected, the resultant spectrum show that new peaks, characteristic of PMMA, appear.

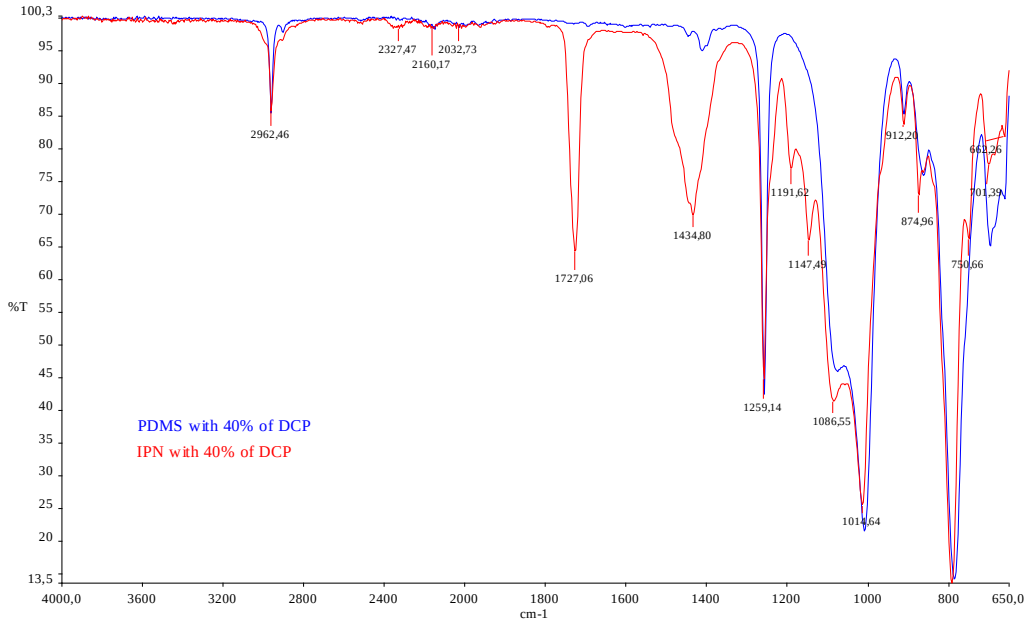

Figure 17 Comparison between the PDMS and the IPN samples with 40 mol% of DCP

According to the figure 18, the amount of PMMA in each sample is different depending on the degree of cross-link although no conclusion can be taken from this fact because a linear behavior is not observed. This result show low quality in the spectrums, perhaps due to the rigidity of the samples analyzed, or some cracks they might had.

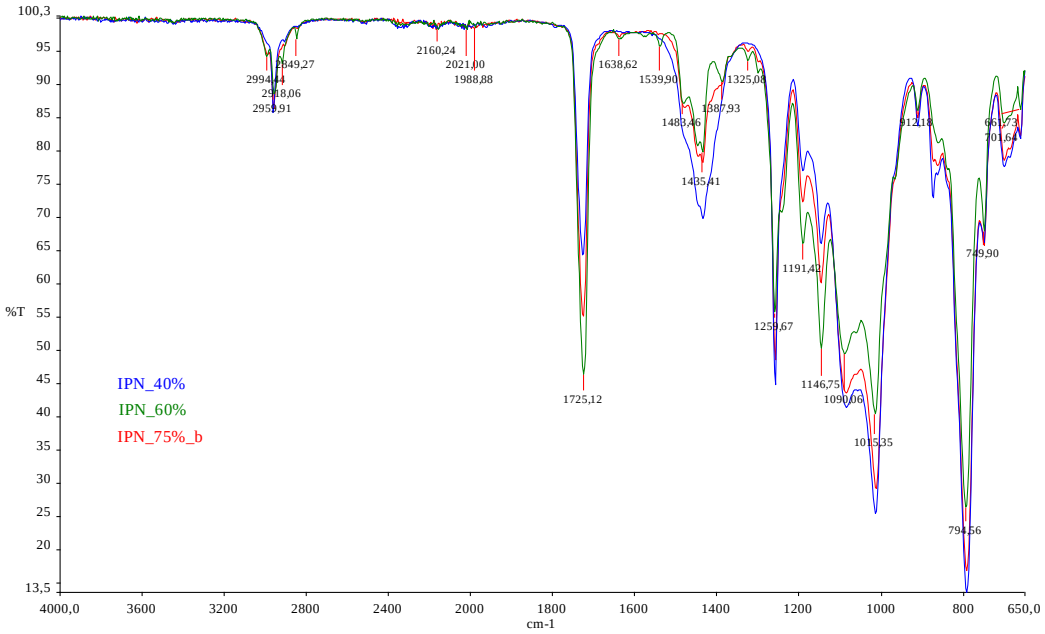

Figure 18 Effect of the amount of cross-linker in the IPN samples

4.3.3 FTIR Measurements of the etched IPN Films

FTIR measurements were done before and after etching the samples. As presented in figure 19, the PDMS peaks do not disappear. Instead they decrease significantly representing a success in the etching procedure

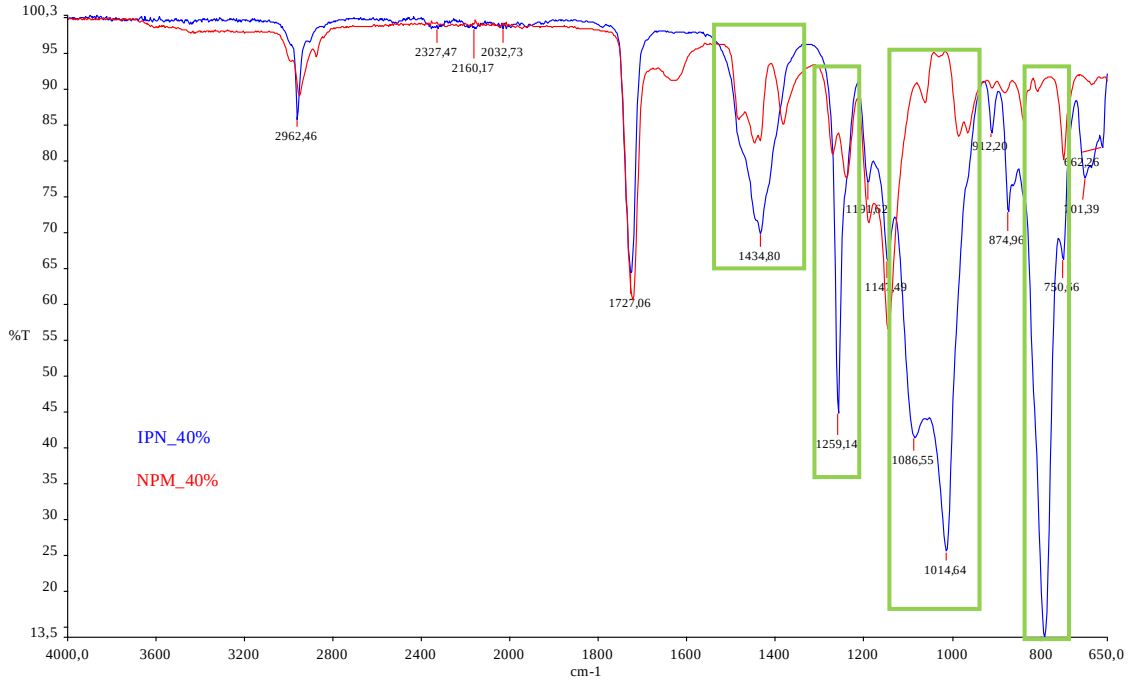

Figure 19 FTIR spectra before and after etching of sample IPN_40 – The PDMS peaks are marked in the green rectangles

4.3.3.1 Etching success

As it was done before for the estimation of the cross-linking success, a quantitative analysis was made to determine the success of the etching procedure.

To determine the etching success of the NPM samples, the ratio between the normalized peak 1014,78 cm^{-1}, characteristic of the Si-O group, in a unetched sample and a etched sample was done. The peak 1727,25 cm^{-1} represents the PMMA group, thus the intensity of this peaks was used as a standard peak, since is not affected by the etching procedure. The FTIR measurements confirm the higher etching success of IPN_60% sample.

Table 11 Etching success

Amount of DCP	Etching success (%)
40 mol %	28,49
60 mol %	86,55
75 mol %	26,46

4.4 Small Angle X-ray Scattering (SAXS)

Electromagnetic radiation can be used to obtain information about materials whose dimensions are on the same order as the radiation wavelength [22]. Small angle scattering of x-ray can be applied to almost all kinds of material, and it is widely used in structural studies of non-crystalline materials at relatively low resolution. The term "small angle" here refers to the angular range within a few degrees, containing structural information on the order of approximately a nanometer to sub micrometers. Many applications of small angle x-ray scattering technique are found in polymer science, colloid chemistry and materials science as well as structural biology [23].

The sample irradiates with a well-collimated beam of some type of radiation, such as x-rays, like showed in figure 20. The resulting intensity, as a function of angle between the incoming beam and scattered beam, is measured and then the structure that originated

the observed pattern is determined [22]. Since x-rays are primarily scattered by electrons, the scattering patterns are caused by the interference of secondary waves that are emitted from electrons. The electrons resonate with the frequency of the X-rays passing through the objects [24]. Scattering of x-rays is caused by differences in electron density. The electrons resonate with a frequency of the x-rays passing through the objects and emit coherent secondary waves, which interfere with each other [24].

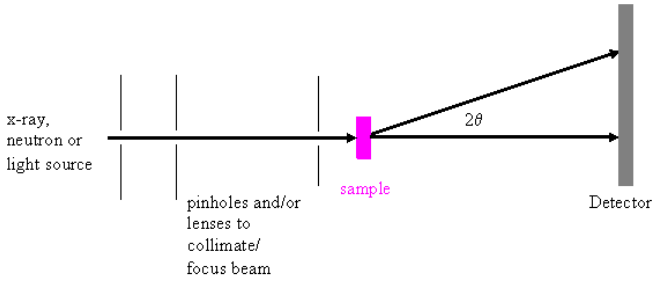

Figure 20 Schematic of x-ray process

Unlike an electron micrograph, small-angle x-ray scattering patterns do not give morphological information directly. The result of a SAXS experiment is essentially the intensity of the Fourier transform of the electron density and must be interpreted in order to determine morphology. One fundamental problem with any scattering experiment is that two different morphologies can, in theory, give identical scattering patterns. Generally, one cannot reconstruct the exact microstructure uniquely from a SAXS pattern because in a scattering experiment only the scattered radiation intensity can be measured and all phase information is lost. Therefore, one cannot be absolutely sure that a scattering pattern is due to a particular morphology.

4.4.1 SAXS Experimental procedure

To analyze the pore system, the samples were placed in a vacuum chamber and exposed to an x-ray beam. The scattering pattern was then captured by the detector. The figure 21 represents the used SAXS set-up.

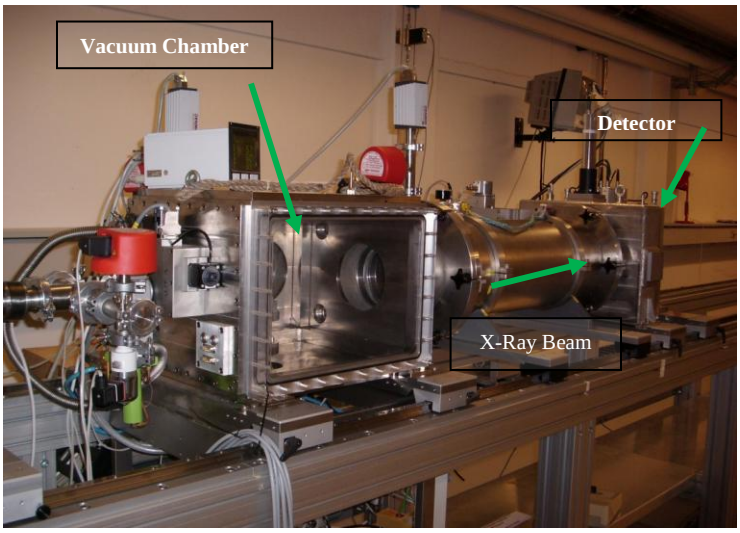

Figure 21 Used SAXS set-up at Risø

General rules for calculating the exposure time cannot be given. Depending in primary beam intensity, scattering power of the sample, type of registration and desired precision of the scattering curve, the measurements of one sample may take from a few minutes (strong scatters like solid polymers) up to several to ten hours (dilute solutions)[24]. In the case of non-porous material the exposure time has to be higher than for a porous one. From previous experience, thirty minutes was the time chosen to analyze the NPM samples, contrasting with the four hours used to study the IPN ones. The selected times to scatter each sample are presented in table 12.

Table 12 Time selected to scatter the samples and the resulting intensity of the beam

Sample	IPN_40	IPN_60	IPN_75	NPM_40	NPM_60	NPM_75
time/ [min]	240	240	240	30	30	30

4.4.2 SAXS Results

The figures above show the scattering images of the IPN_75% and NPM_75%. Both images show the same pattern but the unetched sample is much less intense. The high intensity in the middle is the beam stop on the detector.

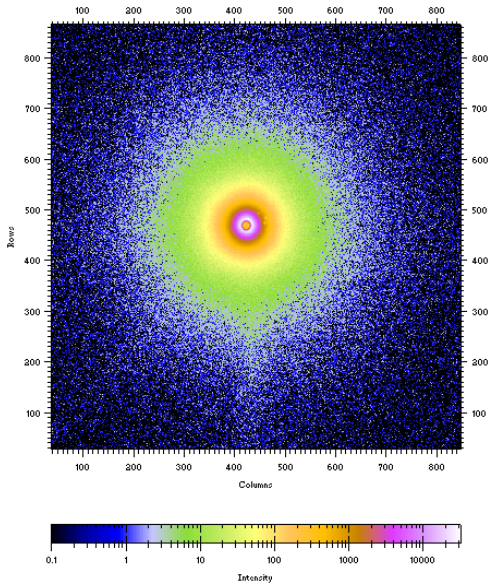

Figure 22 Scattering image of the NPM_75_a

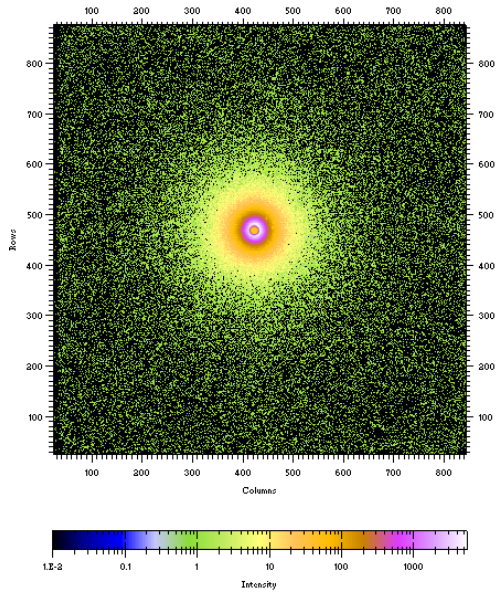

Figure 23 Scattering image of the IPN_75

Since the creation of the PDMS film and the polymerization procedure is random and no self organization effects occur, no regular morphology of the pores is to be expected. The scattering pattern, in figure 24, proofed the idea of a random structure. Otherwise a peak would have occurred in the integrated graph.

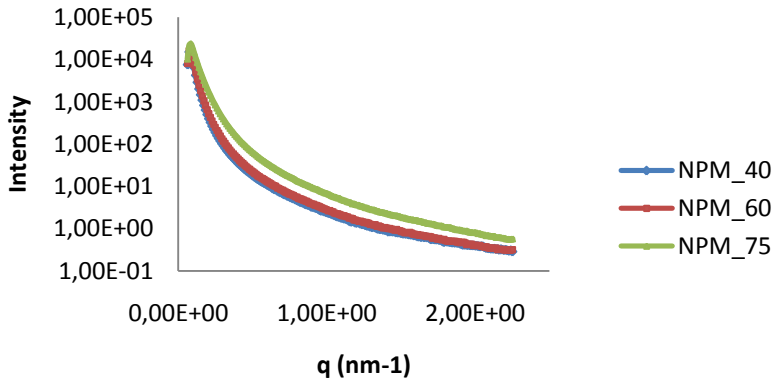

Figure 24 Comparison of the SAXS results for the samples NPM_40, NPM_60 and NPM_75

One way to distinguish a porous from a non porous material is comparing the intensities. The scattering intensity, *I*, is proportional to the square of the difference in electronic density, ρ.

$$I \propto (\rho_2 - \rho_1)^2 \qquad (4.3)$$

Where ρ_2 is the electron density of one component, PMMA, and ρ_1 is the electron density of the other component. If the analysis is being made to a porous material ρ_1 refers to the air and is equal to zero, increasing the scattered intensity. The figure 25 illustrates this relationship, by showing that the NPM has a much higher intensity than the IPN sample.

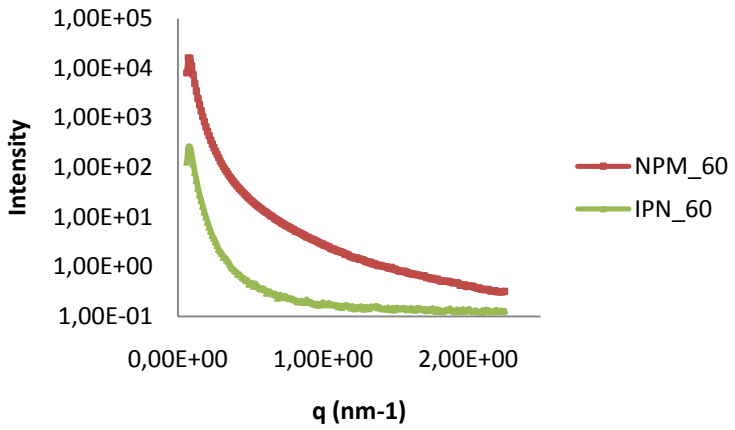

Figure 25 Comparison of the SAXS results for the samples IPN_60 and NPM_60

4.5 Microscopy Methods

Electron microscopy, transmission electron microscopy (TEM) for micro and mesopores samples, and scanning electron microscopy (SEM) for macroporous samples, is an indispensable tool for the investigation of porous materials. The biggest advantage of these techniques is that they deliver an optical image of the samples.

4.5.1 Transmission Electron Microscopy (TEM)

TEM is a microscopy technique where an electron beam is transmitted through an ultra thin specimen interacting with it as they pass through. An image is formed from the interaction of the electrons transmitted through the specimen, which is magnified and focused onto an imaging device.

In order to study the effect of cross-linking degree on the size of the pores, the samples NPM_40, NPM_60 and NPM_75 were prepared in a microtome. The cross

sections of the samples were cut with sizes between 80 to 100 nm. Thus some of the structure can be deformed or cracks can occur.

Since the samples showed to be extremely sensitive to the electron beam, no conclusion about the size of the pores can be made, because they were rapidly being destroyed. On the other hand, the existence of cavities in the porous sample and the inexistence in the non-porous one was clear, as seen in figures 26 and 27.

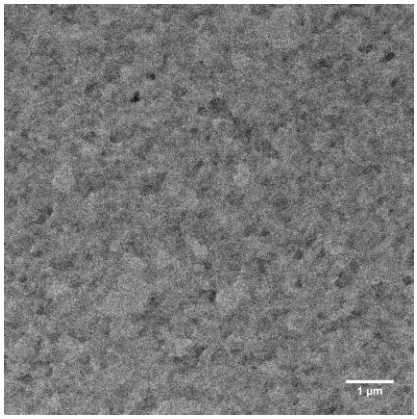

Figure 27 TEM picture of IPN_60

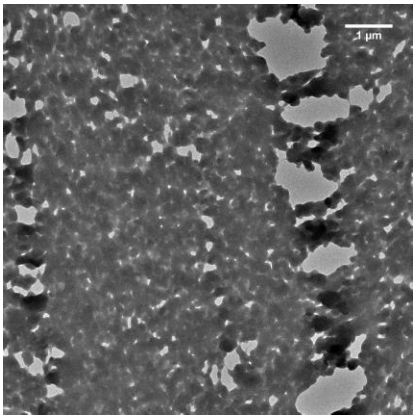

Figure 26 TEM picture of NPM_60

Another interesting remark is that with the increase of the cross-linking degree, the samples became more sensitive to the electron beam.

4.5.2 Scanning electron microscopy (SEM)

The scanning electron microscopy is a type of electron microscope that images the samples surface by scanning it with a high energy beam of electrons in a raster scan pattern. The picture is produced out of interaction of the electrons with the atoms on the sample surface.

The SEM pictures were taken to the cross-sections of the samples NPM_40, NPM_60 and NPM_75, in order to analyze the influence of the cross-linking on the pore size. Some pictures were also taken to the sample IPN_60, to compare the etched with the unetched samples.

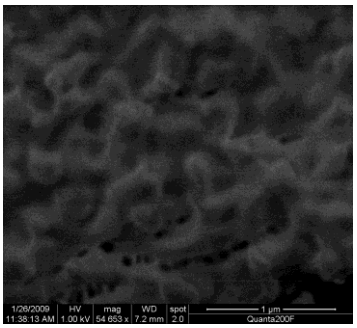

Figure 28 SEM picture of NPM_40

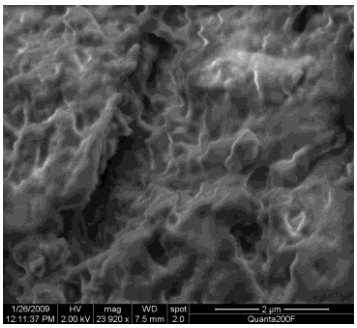

Figure 29 SEM picture of NPM_60

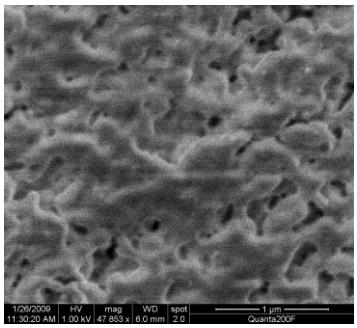

Figure 30 SEM picture of NPM_75

It was expected that, the higher the cross-linking degree the smaller the pores get. The SEM pictures prove that there is no relationship between the cross-linking degree and the size of the pore. In fact the samples NPM_40, although having less number of pores, have sizes between 50 to 100 nm, as NPM_75. The pores of the sample NPM_60 seem to be bigger, with sizes around 400 nm. This fact can also be due to the preparation of the samples, where the cutting could have damaged the samples. Inspite the fact that no relationship between the cross-linking degree and the size of the pores can be concluded, it seems that by increasing the amount of cross-linker, the number of pores also increases.

5 Parallel Work

As referred before the obtained IPN samples are inhomogeneous presenting some parts more transparent than others. As a parallel work a transparent region, IPN_75_a, was analyzed separately from the most opaque region, IPN_75_b. The figure 31 represents a scheme of the sample IPN_75.

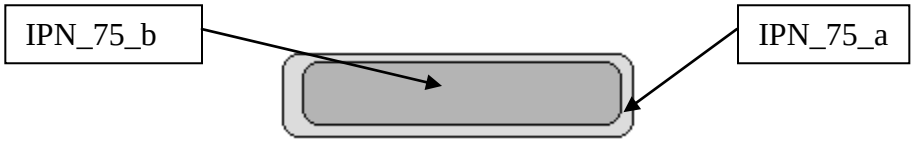

Figure 31 Scheme of the sample IPN_75

5.1 Gravimetric measurements of the samples before and after being etched

Considering that the sample IPN_75_a has the same amount of PDMS that IPN_75_b, the percentage of weight loss was determined and compared to the percentage of the amount of PDMS present in the samples

Table 13 Gravimetric measurements of the samples before and afer being etched

Sample	$w_{before\ etch}$/g	$w_{after\ etching}$/g	Weight loss (w_{before}-w_{after})	Weight loss %	w_{PDMS} % (B. E.)	w_{PDMS} % (A. E.)
75_a	0,066	0,053	0,013	19,301	36,079	16,778
75_b	0,512	0,386	0,126	24,600	36,079	11,479

. Ideally the weight loss should be the same as the amount of PDMS. This situation does not occur, meaning that the etching procedure was not completely done. As one can see in table 13, the weight loss in the most transparent sample was lesser than the most opaque one, being similar to the value obtained for the sample IPN_60 (19,980 % weight loss).

5.2 Methanol Uptake

In order to compare the porosity in the opaque sample to the transparent sample the measure of methanol uptake was preformed and compared with the volume of PDMS removed. The results are presented in figure 32.

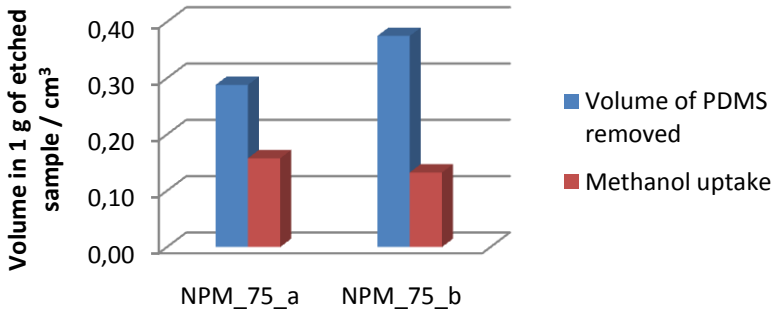

Figure 32 Comparison of methanol uptake and the volume of PDMS removed for the transparent and opaque regions of sample NPM_75

As seen before, the volume of PDMS removed is grater that the methanol uptake for both samples. This result may indicate that the samples were not enough time in contact with methanol. On the other side it was also expected that the volume of methanol uptake in both samples were the same, but instead the most transparent sample has a higher value, indicating that this sample has more available pores.

5.3 FT-IR measurements of the IPN samples IPN_75_a% and IPN_75_b

Comparing the FT-IR spectrums of the samples IPN_75%_a and IPN_75%_b, figure 33, no big difference can be seen. Both samples have the same behavior although the peak corresponding to the PMMA functional group is smaller in the IPN_75%_a sample, the more transparent region. However, analyzing the peak 911cm^{-1} is possible to say that both samples have the same cross-linking degree in the PDMS network.

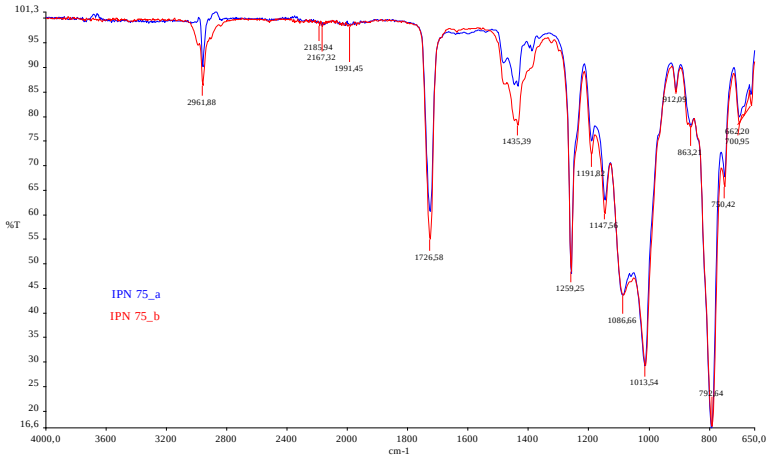

Figure 33 Comparison between the samples IPN_75%_a and b

A quantitative analysis of the FT-IR spectrums was made in order to determine the etching success. This parameter was calculated by the ratio between the normalized peak 1014,78 cm^{-1}, characteristic of the Si-O group, in the unetched sample and the etched sample. The peak 1727,25 cm^{-1} represents the PMMA group, thus the intensity of this peaks was used as a standard peak, since is not affected by the etching procedure.

Table 14 Etching success

Amount of DCP	Etching success (%)
75 mol %_a	27,55
75 mol %_b	26,46

The FTIR measurements show that the etching process has a similar success in both samples. However the most transparent sample, NPM_75_a, has a slightly greater etching success, confirming the results presented in figure 32, in which the values of the volume of PDMS removed and the methanol uptake are closer.

5.3.1 Small Angle X-ray Scattering (SAXS) results

To analyze the pore system of the samples, SAXS images were taken and the data analyzed. As before both samples show a random morphology, otherwise a peak would have occurred in the integrated graph. Another interesting observation is that, comparing the SAXS results for the samples NPM_75_a and NPM_75_b, in figure 34, one can see that both samples show a similar behavior, with much more intensity than the IPN sample.

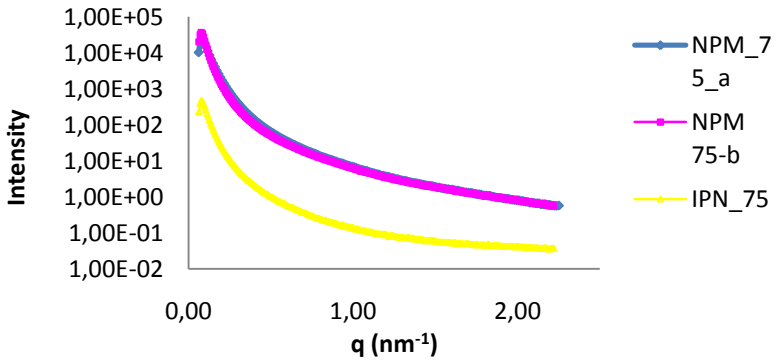

Figure 34 Comparison of the SAXS results for the samples NPM_75_a; NPM_75_b and IPN_75

6 Conclusions and future work

The creation of nanoporous materials out of interpenetrating networks (PDMS-PMMA), by etching a silicone based network with TBAF was done. The interpenetrating networks were produced using a new method [5] where the formation of the IPN was given between two Petri dishes, doused in a mixture of monomer (MMA)/ initiator(AIBN) at 80ºC for two hours after the swelling of a PDMS film with a mixture of MMA/AIBN/DEGMA(cross-linker).

In order to study the effect of the cross-linking degree of the etchable network (PDMS) in the size of the pores of the final nanoporous material, several experiments, such as Gravimetric and swelling measurements, FT-IR, SAXS and microscopy, like TEM and SEM were done to three samples with different amounts of cross-linker (40 mol%, 60 mol% and 75 mol%).

Gravimetric measurements were done to the host network (PDMS), to the interpenetration networks (PDMS-PMMA) and to the final porous material. As it was expected, the increasing of the amount of cross linker makes the swelling ratio, of the PDMS network, decrease. This fact occurs because the higher the cross-linker degree the more rigid is the network offering more resistance to the swelling. On the other hand, unlike it was expected, the cross-linking degree of the host sample did not affect the mass composition of the IPN samples, since, for different amounts of cross-linker the samples presented approximately the same weight percentage of PDMS. One possible answer for this behavior is that the time given to the PDMS to swell the monomer/initiator/cross-linker mixture was probably not enough, not reaching the equilibrium. The different samples were weighted before and after the etching procedure and the percentage of the weight loss was compared with the percentage of the weight of PDMS present in the IPN samples. This experiment showed that the etching procedure was not complete for any of the samples. Furthermore the weight loss did not seem to be affected by the cross linking degree of the host network. On the other hand, the PDMS weight percentage of the sample after being etched decreased with the increase of the cross-linking degree.

A basic method to get a statement about the porosity of a material was done by measuring the methanol uptake. This technique demonstrated that the methanol uptake

decreases with the increase of the PDMS cross-linker degree suggesting with the increase of the cross-linking degree, the pores get smaller, decreasing the methanol uptake. On the other hand, contrasting with what was expected, the volume of PDMS removed was greater than the methanol uptake, suggesting that either the swelling time was not enough to reach the equilibrium or that the PMMA was not sufficiently cross-linked resulting in the collapse of some pores blocking the methanol uptake in some regions.

. A quantitative FTIR analysis made possible the determination of the success of the cross-linking and etching processes. In neither the cases a conclusion about the effect of cross-linking degree of the samples and the success of both procedures, could be done. The sample with 40 mol% of DCP was showed a more successful cross-linking procedure, although all the samples had a good value of this parameter. Then again the FTIR measurements demonstrated that the sample that presented a higher etching success was the sample with 60 mol% of cross-linker.

The SAXS scattering images proved that the IPN creation is random and no self organization effects occur. Furthermore it became clear that the porous samples have a higher scattering intensity than the non-porous ones, proving the existence of cavities.

TEM experiments were unsuccessful since the samples showed to be extremely sensitive to the electron beam. On the other hand, the existence of cavities was clear, but, because the samples were being destroyed no measure could be made. Another interesting remark is that with the increase of the cross-linking degree, the samples became more sensitive to the electron beam.

It was expected that, the higher the cross-linking degree the smaller the pores get. The SEM pictures prove that there is no relationship between the cross-linking degree and the size of the pore. In fact the samples NPM_40, although having less number of pores, have sizes between 50 to 100 nm, as NPM_75. The pores of the sample NPM_60 seem to be bigger, with sizes around 400 nm. This fact may also be due to the cutting procedure where the samples could have been damaged.

The obtained IPN samples were inhomogeneous presenting some parts more transparent than others. As a parallel work a transparent region was analyzed separately and compared from the most opaque region. Gravimetric measurements demonstrated that the etching procedure was not complete. Both samples had different results for the

methanol uptake, being the most transparent region the one with a higher value and a smaller difference between the volumes of PDMS removed and the methanol uptake. As before, SAXS pictures indicate a random morphology.

Resuming what was said above, no conclusion on a relationship between the cross-linking degrees on the size of the pores can be taken and the produced samples show random polymerization, random morphology and sizes. Furthermore, if on one hand we saw that the methanol uptake decreases with the increase of the x-linking degree and on the other hand is suggested, by SEM pictures, that the increase of cross-linking degree increases the number of pores, is suggested that a possible collapse of some pores may have occurred.

6.1 Future work

Diffusion effects seemed to occur during the polymerization of MMA from the host network to the surroundings. Thus, in order to control the sample composition and the PMMA cross-linking degree, some changes in the Petri dish sandwich method was tested. In this changed technique, the exactly same mixture used to swell the host network was added to the Petri-Dish, along with the sample, and placed in the oven to polymerize at 80ºC. Preliminary results seem to be successful, since the separation of the PMMA in the surrounding of the IPN structure was, as previously, very easy to perform becoming a big advantage of that method.

From Gravimetric measurements we can conclude that, as before, with the increasing of temperature, the sample continues to swell the surrounding mixture, but this time, with the advantage of knowing the exact composition.

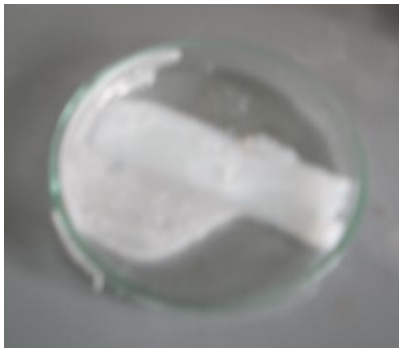

Figure 35 IPN sample before being removed from the Petri dish

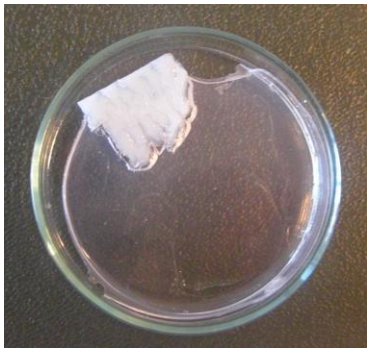

Figure 36 IPN_77 mol% made by the changed Petri dish method

As future work, the effect of cross-linking degree, of the host network, on the size of the pores should be done using the changes suggested in the parallel work. As an alternative, in order to for create PDMS/PMMA interpenetration networks the monomer immersion method described in [10] [11][12] should be used, with the advantage of having already several studies made allowing a higher control on the process.

On the other hand, for a better understanding of the IPN formation behavior the gravimetric analysis should be done with methacrylates instead of cyclohexane, in order to insure a greater control on the process.

The effect of other parameters, such as pH, the swelling time and PMMA's cross-linking degree, in the size of the pores should also be studied. The time used to swell the PDMS film in a mixture of MMA/initiator/cross-linker is an important parameter and is suggested to be, in a first stage, of 18 hours, as indicated in several reports in which the monomer immersion method is used. The IPN morphology was found to be pH-dependent [12], thus the influence with the final porous material should also be investigated. The relationship between the success of the etching procedure and the PMMA's cross-linking success should also be studied. To further understand the properties of the porous materials a set of experiments should be established to study the swelling behavior, permeability, morphology and mechanical properties of these NPM.

It would also be interesting to test this method various networks, such as gelatin, that can be easily removed with hot water.

References

[1]. Lu, G.Q.; Zhao, X.S.; Nanoporous materials – Science and Engineering; 2004

[2]. Guo F.; Andreasen J. W.; Vigild M. E.; Ndoni S.; Influence of 1,2-PB Matrix Cross-linking on structure and Properties of selectively Etched 1,2-PB-b-PDMS Block copolymers; 2007

[3]Vigild M.E.; Ndoni S.; Berg R.H; Nano-porous Elastomers based on Polymer self assembly

[4] Sperling L.H.; Interpenetrating Polymer Networks; Encyclopedia of polymer Science and Technology, 2004

[5].Andreas F. Janus; Maximilian B. Schneider; Creating Nanoporous materials out of commercial available substances in an Economic Process; 2008

[6] http://www.nanoroadmap.it/, seen in January 7th, 2009

[7]Cohen Y., and Peters E.W., Novel adsorbents and their environmental applications, AICHE symposium Series, 91 (1995) New York

[8]Yang RT., Adsorbents: Fundamentals and Applications; 2003, Brisbane, John Wiley & Sons, Inc.

[9]Xing W., Yan Z.F., Ryoo R. and Lu G. Q., Advanced Materials, submitted, 2003

[10] J.S. Turner, Y.-L. Cheng, Preparation of PDMS–PMAA IPNs using the monomer-immersion method, Macromolecules 33 (10) (2000) 3714–3718.]

[11] J.S. Turner, Y.-L. Cheng, Morphology of PDMS–PMAA IPN membranes, Macromolecules 36 (6) (2003) 1962–1966.]

[12] J.S. Turner, Y.-L. Cheng;; Ph dependence of PDMS-PMMA morphology and transport properties , journal of membranes Science, 240 (2004) 19-24]

[13]S. Ndoni, M. E. Vigild, R. H. Berg, *J. Am. Chem. Soc.* **2003**, *125* , 13366]
[14]M. S. Hansen, M. E. Vigild, R. H. Berg, S. Ndoni, *Polym. Bull.* **2004**, *51* , 403

[15] He. X. W.; Widmaier J. M. ; Herz J. M. and Meyer G. C.; Polydimethylsiloxane/poly(methyl methacrylate) interpenetrating polymer networks: 2. Synthesis and properties;1992

[16]Turner J.S.; Cheng Y.L.; Morphology of PDMS-PMMA IPN membranes; 2003

[17]Turner J.S.; Cheng Y.L.; Preparation of PDMS – PMMA interpenetrating polymer network membranes using the monomer immersion method; 2000

[18] Dong J.; Liu Z. L.; Wang Q.; Preparation, Morphology and mechanical properties of elastomers based on alfa, omega-dihidroxy-polydimethylsiloxane; 2004

[19] Clayden, Greeves, Warren and Wothers; Organic Chemistry; 2001

[20] http://www.thermo.com/eThermo/CMA/PDFs/Articles/articlesFile_12268.pdf; seen in December 1st, 2008

[21]Pavia, Lampman, Kriz; Introduction to spectroscopy – third edition; 2001

[22] http://coecs.ou.edu/Brian.P.Grady/saxs.html; seen in December 12th, 2008

[23] http://www-ssrl.slac.stanford.edu/saxs/saxs.html; seen in December 12th, 2008

[24] Glatter, O. & Kratky, O., eds. Small Angle X-ray Scattering; Academic Press, 1982

Appendixes

Appendix A

Calculations made to the preparation of samples:

Determination of the desired amount of the host network (PDMS)

$$w(PDMS) = \frac{\pi}{4} d^2 \times t \times \rho \qquad \text{(A.1)}$$

Where d is the diameter of the Petri dish (5, 5 cm), t is the desired thickness (0,15 cm) and ρ the density of the polymer (0,97g/cm^3). With these values the amount of PDMS obtained is:

Determination of the needed amount of cross-linker (DCP)

According to the following scheme the active element was considered to be the group methyl hidro siloxane $HSiOCH_3$. (*M (Active Group)* =60.08 g/mol)

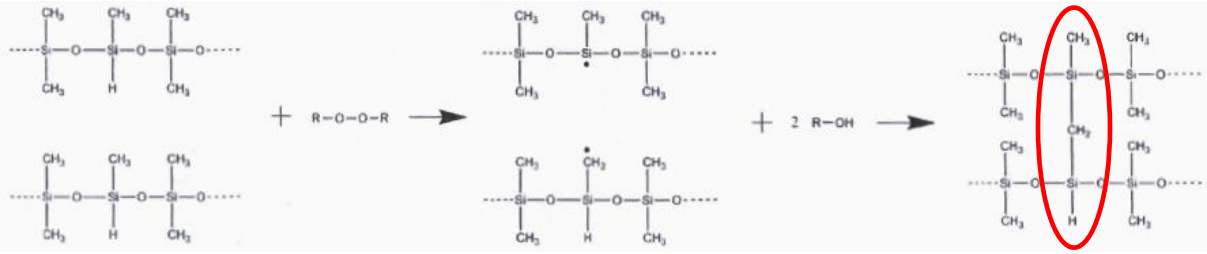

Figure 37 Reaction scheme of the radical cross linking

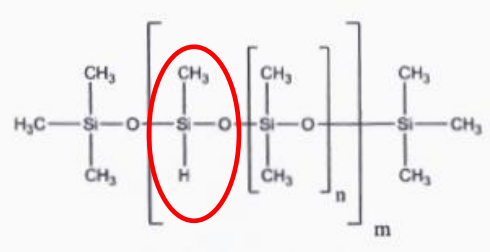

Figure 38 Structure of the Methylhydro dimethyl siloxane; n/m=30

In the figure 28, the active chain is marked in the green rectangle and is considered to be the polymeric chain between two successive cross links.

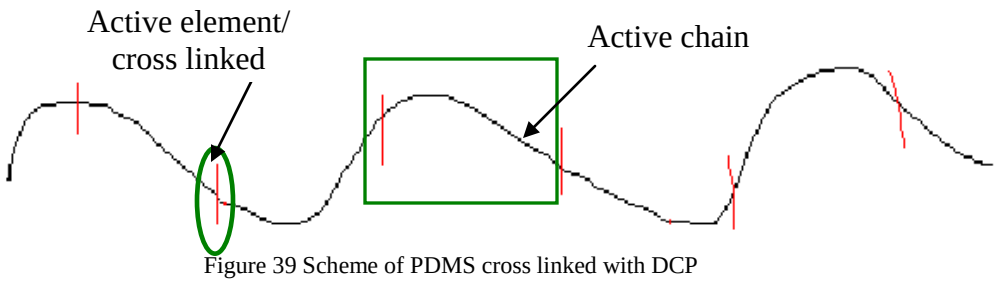

Figure 39 Scheme of PDMS cross linked with DCP

The molar percentage of cross-linker used was defined as:

$$(DCP)mol\% = \frac{n(DCP)}{n(Activechain)} \times 100 \qquad \textbf{(A.2)}$$

With this definition, the amount of DCP can be calculated in the following way:

$$w(DCP) = DCP\ mol\% \times \frac{w(commercial\ \ PDMS)}{M(active\ \ chain)} \times M(DCP) \qquad \textbf{(A.3)}$$

The molecular weight of active chain per active group *M (Active chain)* can be determined in the subsequent way:

$$M\left(activechain\right) = \frac{mol\%(activegroup)}{mol\%(activegroup)} \times M\left(HSiOCH_3\right) + \frac{1 - mol\%(activegroup)}{mol\%(activegroup)} \times M\left(SiO(CH_3)_2\right) \qquad \textbf{(A.4)}$$

Where, considering the Molecular weight of ($HSiOCH_3$) and the molecular weight of $SiO(CH_3)_2$ as 60,08 and 74,08 g/mol, respectively, the mol%(active group) is given by:

$$mol\%(active\ group) = \frac{\frac{w(PDMS)}{M(HSiOCH_3)}}{\frac{w(PDMS)}{M(HSiOCH_3)} + \frac{1-w(PDMS)}{M(SiO(CH_3)_2)}} \qquad \textbf{(A.5)}$$

According to the manufacturer the copolymer has 3 to 4% of methyl-hidro-siloxane groups. Thus, I considered that in the commercial polymer there is 3.5 wt% of PDMS (w(PDMS in the commercial polymer)=0,035g). From the last equation the mol% (active group) is 0,04281. And consequently the *M(active chain)* is 1716,571 g/mol of active group.

Appendix B

Calculations made to analyze the samples:

Gravimetric measurements

IPN's composition

The weight percentage of each network, in the IPN samples was calculated as the following:

$$w\%\ (PDMS) = \frac{w(PDMS)_{before\ \ swell}}{w(IPN)} \times 100 \quad \textbf{(B.1)}$$

$$w\%\ (PMMA) = \frac{w_{IPN} - w(PDMS)_{IPN}}{w_{IPN}} \times 100 \quad \textbf{(B.2)}$$

NPM's composition

The etched mass was determined by:

$$w(sample)_{before\ \ etch} - w(sample)_{after\ \ etch} \quad \textbf{(B.3)}$$

And the percentage of weight loss by:

$$\%weight\ loss = \frac{etch weight\ loss}{mass\ \ before\ \ etch} \times 100 \qquad \textbf{(B.4)}$$

The percentage of PDMS that remained in the porous material was calculated by:

$$\%w(PDMS)_{NPM} = \%w(PDMS)_{IPN} - \%weight\ loss \qquad \textbf{(B.5)}$$

FT-IR quantitative analysis

The image bellow is an example to illustrate of different peaks in a FT-IR spectrum

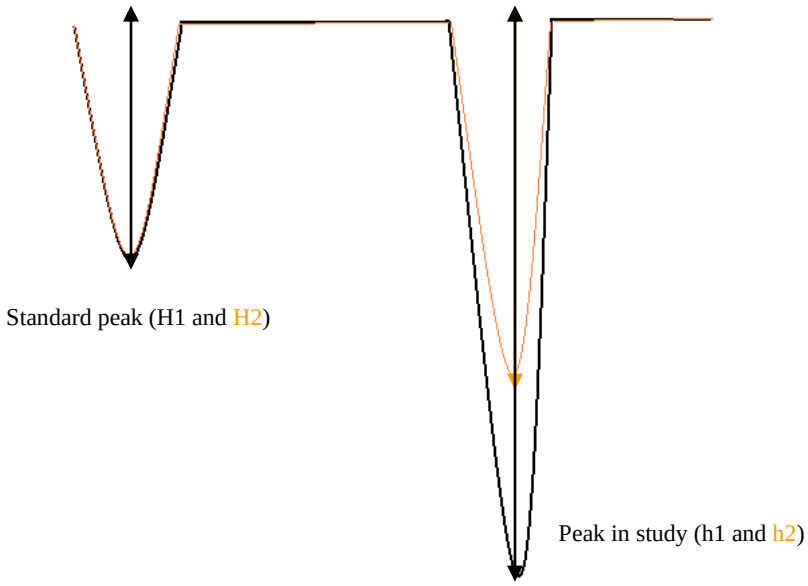

Figure 40 Scheme of two overlapping FTIR spectrums

Cross-linking – FT-IR quantitative analysis

The table above shows the height of the peaks, 1256,06 and 911,38 cm^{-1}, before and after the cross-linking procedure for the samples PDMS_40%, PDMS_60% and PDMS_75%.

Table 15 Height of the peaks, 1256,06 and 911,38 cm^{-1}, before and after the cross-linking procedure

	Hight (%T)			
Peak	**PDMS 0% of DCP (1)**	**PDMS 40 (2)**	**PDMS 60 (2)**	**PDMS 75 (2)**
1256,06 (H)	41,15	43,05	36,98	39,34
911,38 (h)	78,6	85,25	85,07	84,35

The cross-linking success was obtained using the equation above:

$$\%\, x - linking = \frac{\frac{h_1}{H_1}}{\frac{h_2}{H_2}} \times 100 \quad \textbf{(B.5)}$$

Where the index 1 represents the intensity (%T) of the peak of the sample without cross-link (PDMS_0%), and the index 2 represent the intensity of the peaks of the cross-linked samples.

Etching – FT-IR quantitative analysis

The table above shows the height of the peaks 1724,25 and 1014,78 cm-1, before (IPN_40% , IPN_60% , IPN_75_a% IPN_75b%)and after etching the samples (NPM_40% , NPM_60% , NPM_75_a% NPM_75b%)

Table 16 Height of the peaks, 1724,25 and 1014,78 cm-1, before and after etching the samples

	Height (% T)							
Peak (cm^{-1})	**IPN 40**	**NPM 40**	**IPN 60**	**NPM 60**	**IPN 75_a**	**NPM 75_a**	**IPN 75_b**	**NPM 75_b**
1724,25 (H)	65,63	60,63	46,49	98,56	61,63	54,99	56,18	47,24
1014,78 (h)	29,33	95,12	40,51	99,23	29,33	94,98	29,33	93,2

The etching success was obtained using the equation above:

$$\%\ etching\ success = \frac{\frac{h_1}{H_1}}{\frac{h_2}{H_2}} \times 100 \quad \textbf{(B.6)}$$

Where the index 1 represents the intensity (%T) of the peak of the unetched sample (IPN) and the index 2 represent the intensity of the peaks of the etched samples (NPM)